A Sharp Maxwell Bound for Three Point Charges

Shiva Kintali*

August 1, 2026

Abstract

Let $a_1, a_2, a_3 \in \mathbb{R}^3$ be distinct and let $q = (q_1, q_2, q_3) \in (\mathbb{R} \setminus \{0\})^3$. We prove that the Coulomb potential $V_q(x) = \sum_{i=1}^{3} q_i/|x - a_i|$ has at most four distinct critical points whenever its critical set is finite. Our bound is sharp. No nondegeneracy assumption is imposed, so isolated degenerate equilibria are included. We improve the bound to two for collinear sites and to three for noncollinear sites with $\sum_i q_i = 0$. Our proof combines a projective charge map, four elliptic discs, an exact Lami identity, degree theory, a cusp count, and an injectivity theorem for anti-periodic support envelopes.

1 Introduction

For point charges of strengths q_i at distinct sites $a_i \in \mathbb{R}^3$, the electrostatic potential is

$$V_q(x) = \sum_{i=1}^{n} \frac{q_i}{|x - a_i|}, \qquad x \in \mathbb{R}^3 \setminus \{a_1, \ldots, a_n\}.$$

In the 1873 first edition of his *Treatise*, Maxwell tracked changes in the periphraxy and cyclosis of equipotential regions and counted points or lines of equilibrium according to their degrees. He asserted, without proof, that for charged points or spherical conductors the number of additional equilibria arising through cyclosis cannot exceed $(n-1)(n-2)$, where n is the number of bodies [10]. The third edition, edited by J. J. Thomson and published in 1892, contains Thomson's bracketed footnote stating that he had been unable to find a proof of the estimate [11]. Gabrielov, Novikov, and Shapiro explained how Maxwell's weighted counts and this auxiliary estimate lead to the bound $(n-1)^2$, and formulated the modern conjecture for configurations whose equilibria are all nondegenerate [5].

For the generalized potentials $V_\alpha(x) = \sum_i \zeta_i/|x - a_i|^{2\alpha}$, $\alpha > 0$, Gabrielov, Novikov, and Shapiro proved the upper bound 12 for every nondegenerate three-charge configuration, allowing arbitrary signs; the Coulomb potential is the case $\alpha = 1/2$ [5]. Tsai proved the four-equilibrium bound for the planar problem when the three sites form an equilateral or isosceles right triangle [14]. He later treated arbitrary three-site configurations with equal charge magnitudes: when the critical set is finite, the number of isolated equilibria is at most four, and the exceptional configurations with infinitely many equilibria are classified [15]. Related complex-analytic treatments of planar charges, including an application of the argument principle to the three-charge problem, appear in [9, 12].

Zolotov obtained the general bound $5 \cdot 9^{n+3}$ for the number of isolated Coulomb critical points [17]. Edelsbrunner, Fillmore, and Oliveira subsequently obtained the bound $2^n(3n-2)^3$ for a generic position of one site, with the remaining sites and all nonzero strengths fixed [4]. Arathoon, Ball, and Kvalheim constructed five positive charges whose potential has at least 24 nondegenerate critical points. They further showed that an arbitrarily small perturbation of the strengths gives a finite

*Email: shiva.kintali@gmail.com Homepage: shivakintali.github.io

critical set of cardinality at least 24, all of whose points are nondegenerate, thereby disproving the general Maxwell conjecture [1]. They also noted that the three-charge problem was not known beyond Tsai's equal-magnitude cases [1]. In a 2026 preprint, Gabrielov, Dm. Novikov, T. Novikov, and Shapiro improved the upper bound from 12 to 6 for three positive charges with nondegenerate equilibria [6].

In this paper, we give the first sharp upper bound of four equilibria for arbitrary configurations of three distinct sites and arbitrary nonzero real strengths, assuming only that the critical set is finite.

Theorem 1 (Three-charge Maxwell bound). *Let $A = \{a_1, a_2, a_3\} \subset \mathbb{R}^3$ consist of three distinct points, let $q \in (\mathbb{R} \setminus \{0\})^3$, and define*

$$V_q : \mathbb{R}^3 \setminus A \longrightarrow \mathbb{R}, \qquad V_q(x) = \sum_{i=1}^{3} \frac{q_i}{|x - a_i|}.$$

Define the critical set by

$$\mathrm{Crit}(V_q) := \{x \in \mathbb{R}^3 \setminus A : \nabla V_q(x) = 0\}.$$

If this set is finite, then $\#\,\mathrm{Crit}(V_q) \leq 4$, the points being counted without multiplicity; see Remark 1.1 for sharpness. Moreover, $\#\,\mathrm{Crit}(V_q) \leq 2$ if the sites are collinear, and $\#\,\mathrm{Crit}(V_q) \leq 3$ if the sites are noncollinear and $\sum_i q_i = 0$.

Remark 1.1 (Sharpness). The constant 4 is sharp: three equal positive charges at the vertices of an equilateral triangle have four nondegenerate equilibria [15]; see also [1]. The collinear constant 2 is sharp. Indeed, take equal positive charges at $a_i = (h_i, 0)$ with $h_1 < h_2 < h_3$, and write a point as $x = (t, y) \in \mathbb{R} \times \mathbb{R}^2$. The transverse component of the equilibrium equation is $y \sum_i q_i / |x - a_i|^3 = 0$. Its scalar factor is positive, so $y = 0$. After division by the common charge, the axial field is

$$E(t) = \sum_{i=1}^{3} \frac{t - h_i}{|t - h_i|^3}.$$

It has derivative $E'(t) = -2 \sum_i |t - h_i|^{-3} < 0$ on each gap and tends from $+\infty$ to $-\infty$ across that gap; it has a fixed sign on each exterior interval. It therefore has exactly one zero in each gap and none elsewhere. By contrast, it is not known whether the constant 3 in the noncollinear zero-sum case is attained. Remark 9.3 derives an explicit necessary condition for attainment, proves restrictions on that condition, and formulates the stronger conjecture that every noncollinear zero-sum configuration with finite critical set has exactly one equilibrium.

The finiteness hypothesis is necessary for a literal cardinality statement with signed charges. For example, take sites

$$a_1 = (-1, 0, 0), \qquad a_2 = (0, 0, 0), \qquad a_3 = (1, 0, 0)$$

and strengths $(-2\sqrt{2}, 2, -2\sqrt{2})$. At every point $x = (0, y, z)$ with $y^2 + z^2 = 1$, the three distances are $(\sqrt{2}, 1, \sqrt{2})$ and the coefficients $q_i / |x - a_i|^3$ are $(-1, 2, -1)$. Consequently,

$$\sum_i \frac{q_i (x - a_i)}{|x - a_i|^3} = -(x - a_1) + 2(x - a_2) - (x - a_3) = a_1 + a_3 - 2a_2 = 0.$$

Since ∇V_q is the negative of this sum, the entire unit circle is critical. Thus the finiteness hypothesis cannot be omitted for arbitrary signed strengths. The theorem makes no assertion about configurations with positive-dimensional critical sets, and the hypothesis is weaker than nondegeneracy because isolated degenerate critical points are allowed. For the modern nondegenerate formulation, finiteness is automatic. Indeed, introduce variables $r_i > 0$ with $r_i^2 = |x - a_i|^2$. After multiplication by $\prod_i r_i^3$, the equations $\nabla V_q(x) = 0$ are polynomial in (x, r_1, r_2, r_3). The critical set is exactly the projection onto x-space of the semialgebraic set defined by these polynomial equations, the equations $r_i^2 = |x - a_i|^2$, and the inequalities $r_i > 0$. It is therefore semialgebraic by the Tarski–Seidenberg theorem. Nondegeneracy makes each of its points isolated, and each isolated point is a connected component. Since a semialgebraic set has only finitely many connected components, the critical set is finite.

1.1 Notation

Throughout, $A = \{a_1, a_2, a_3\}$ and $q = (q_1, q_2, q_3)$ with every $q_i \neq 0$. When the sites are noncollinear, write P for their affine plane. We fix the labelling and choose the orientation of P so that

$$S = \tfrac{1}{2} \det(a_2 - a_1,\, a_3 - a_1) > 0.$$

Every subsequent relabelling is cyclic and therefore preserves this convention. Choose Euclidean coordinates compatible with this orientation and identify P with $\mathbb{C}$. Set $P_A = P \setminus A$. For $x \in P_A$, write

$$u_i = x - a_i = r_i e^{i\alpha_i}, \qquad e_i = \frac{u_i}{\bar{u}_i} = e^{2i\alpha_i}.$$

Here $r_i = |x - a_i| > 0$. The symbol ∇ denotes the ambient three-dimensional gradient, whereas ∇_P denotes the planar gradient. Unless explicitly stated otherwise, Hessians, local indices, and winding numbers in the noncollinear argument are taken in the oriented plane P.

The following symbols are used with a fixed meaning throughout.

λ_i	normalized barycentric coordinates	$\Xi = \sum_i \lambda_i e_i$	shape function
$\vartheta(x) = (\lambda_i r_i^3)_i$	canonical charge	$\Theta = [\vartheta]$	projective charge map
$\mathcal{R} = \{\lvert\Xi\rvert < 1/3\}$	planar-index-+1 region	Ω	one component of $\mathcal{R}$
$T = \operatorname{conv} A$, $\widehat{T}$	triangle, vertex blow-up	φ_i	interior angle of T at a_i
L_i, $\ell_i = \sqrt{L_i}$	side lengths squared, side lengths	y_i	Ravi variables
$\mathcal{V}$, $\mathcal{T}$	Jacobian numerator, AM–GM tail	(s,t)	edge-chamber chart
$\mathcal{Q}_i$, $\mathcal{Q}$	$(\sum_j \hat{\lambda}_j)^2 r_i^2$, $\prod_i \mathcal{Q}_i$	Φ, $\mathcal{L}$	$\mathcal{H}$-numerator, fold polynomial
$\mathcal{H} = 1 - \lvert\Xi\rvert^2$	shape deficit	$\mathcal{E}$, $\mathcal{S}$	edge-fold eliminants
ψ, $\beta_i = \alpha_i - \psi/2$	fold phase, reduced angles	$t_i = \tan\beta_i$	tangent chart on the fold
$n, \widehat{n}, \widetilde{n}$	Lami covectors	ν	canonical charge vector
$\mathfrak{a}, \mathfrak{b}$	Lami coefficients		
σ, D_σ, E	sign vector, sign and chart matrices	$\mathbf{N}$, c_{aff}	dual-line normal and offset
h, $\rho = h + h''$, Γ	support, speed factor, envelope	θ	normal angle
θ_i, c_i, s_i	directions $x_0 \to a_i$, cosine, sine	$\mathfrak{d}_i$, $\mathfrak{D}$	$\sin(\theta_k - \theta_j)$, their product
$\mathfrak{p}_i$	$2c_j c_k + s_j s_k$	$\mathsf{e}_1, \mathsf{e}_2, \mathsf{e}_3$	symmetric functions of the t_i
$\mathfrak{N}$, $\mathfrak{s}$, m, d	total, outer, interior, boundary counts	w_∞	outer-field winding

1.2 Proof strategy

The noncollinear proof is in Sections 2–9 and has four stages. First, a projective charge map Θ identifies equilibria with fibres over charge rays, and a complex shape function Ξ identifies the singular locus of Θ (Section 2). Second, the region $|\Xi| < 1/3$ is shown to consist of four discs, one in each allowed barycentric sign chamber (Section 3). Third, an exact Lami identity proves that the dual normal of each caustic turns monotonically (Sections 4–6). A fourth-order calculation classifies the boundary singularities as folds or ordinary cusps, and a projective-degree argument shows that each fold circle carries exactly three cusps (Section 7). An anti-periodic support-envelope lemma then makes each caustic a Jordan curve (Section 8). Finally, Brouwer degree and the planar gradient index formula give the bound (Section 9). Collinear sites are handled separately in Section 9.1 by zonal harmonic expansions.

The longer polynomial identities are computer-assisted but exact, and each one is reconstructed from displayed definitions. The two largest certificate polynomials, $\mathcal{V}$ and $\mathcal{S}$, are constructed explicitly in Section 3. The AM–GM certificate for $\mathcal{V}$ and the full coefficient list for $\mathcal{S}$ are recorded in Appendices A and B, respectively. The remaining proof-critical identities and the complete assertion-based certificate suite are described in Section 10.

2 Planarity and the charge map

Throughout this section, the sites are noncollinear. Let $\vec{P}$ denote the translation plane parallel to P; thus $T_xP = \vec{P}$ for every $x \in P$.

Lemma 2.1 (Planarity)**.** *$\mathrm{Crit}(V_q) \subset P$, and $\mathrm{Crit}(V_q)$ is exactly the zero set of $\nabla_P V_q$ on P_A, where ∇_P denotes the gradient of the restriction $V_q|_P$.*

Proof. Write $x = (x_P, z)$ after choosing $P = \{z = 0\}$, and set $m_i = q_i/|x - a_i|^3$, so that $\nabla V_q(x) = -\sum_i m_i(x - a_i)$. If $\nabla V_q(x) = 0$ and $z \neq 0$, the normal component gives $\sum_i m_i = 0$ because every a_i has vanishing normal coordinate; the tangential component then gives $\sum_i m_i a_i = (\sum_i m_i)x_P = 0$. Thus (m_1, m_2, m_3) is an affine dependence among a_1, a_2, a_3. The sites are affinely independent in P, so every m_i vanishes, contrary to $q_i \neq 0$. Hence every equilibrium lies in P. Conversely, V_q is invariant under the reflection fixing P, so its normal derivative vanishes identically on P; therefore the zeros of $\nabla_P V_q$ are exactly the three-dimensional equilibria. ☐

For $x \in P_A$ let $\lambda_i = \lambda_i(x)$ be the normalized barycentric coordinates, characterized by

$$\sum_i \lambda_i = 1, \qquad \sum_i \lambda_i u_i = 0,$$

equivalently $x = \sum_i \lambda_i a_i$; they exist and are unique because the sites are affinely independent. Since $\sum_i \lambda_i = 1$, the vector λ never vanishes, and neither does $\vartheta(x) = (\lambda_1 r_1^3, \lambda_2 r_2^3, \lambda_3 r_3^3)$.

Some entries of the canonical vector $\vartheta(x)$ may vanish when x lies on one of the lines $L_{ij} := \mathrm{aff}\{a_i, a_j\}$. Such zero-coordinate vectors are used only as auxiliary charge parameters, outside the standing assumption $q \in (\mathbb{R} \setminus \{0\})^3$; the formula for V_q and all of its derivatives extends without change to every $q \in \mathbb{R}^3 \setminus \{0\}$.

Lemma 2.2 (Charge map)**.** *The map $\Theta : P_A \to \mathbb{RP}^2$, $\Theta(x) = [\vartheta(x)]$, is well defined and real analytic. For every $x \in P_A$,*

$$x \in \mathrm{Crit}(V_q) \iff [q] = \Theta(x) = [\lambda_1 r_1^3 : \lambda_2 r_2^3 : \lambda_3 r_3^3]. \tag{2.1}$$

Proof. The preceding paragraph shows that ϑ never vanishes, so Θ is well defined; its real analyticity follows from $r_i > 0$ on P_A. Criticality means $\sum_i (q_i/r_i^3)u_i = 0$. The linear map $\mathbb{R}^3 \to \vec{P}$, $c \mapsto \sum_i c_i u_i$, has rank two. Indeed, a smaller rank would make all three u_i parallel, forcing x and the three sites to be collinear. Its kernel is therefore one dimensional and contains the nonzero vector λ; hence the kernel is $\mathbb{R}\lambda$. Thus $\sum_i (q_i/r_i^3)u_i = 0$ if and only if $q_i = \varsigma \lambda_i r_i^3$ for some $\varsigma \neq 0$. ☐

Define

$$\Xi(x) = \sum_i \lambda_i e_i = \sum_i \lambda_i e^{2i\alpha_i}, \qquad \mathcal{R} = \{x \in P_A : |\Xi(x)| < 1/3\}.$$

Closures and boundaries of subsets of P_A in this section are taken relative to P_A. For $\sigma \in \{\pm 1\}^3$, a *strict barycentric sign chamber* is a nonempty set $C_\sigma = \{x \in P_A : \operatorname{sign} \lambda_i(x) = \sigma_i \text{ for } i = 1, 2, 3\}$. Each C_σ is convex because the barycentric coordinates are affine.

Lemma 2.3 (Hessian and singular locus). *Fix $x \in P_A$. For the canonical representative $q = \vartheta(x)$, the planar Hessian of V_q at x is*

$$H_0(x) = \tfrac{1}{2}\big(I + 3\mathsf{M}(\Xi(x))\big), \qquad \mathsf{M}(z) = \begin{pmatrix} \Re z & \Im z \\ \Im z & -\Re z \end{pmatrix}. \tag{2.2}$$

If $q = \varsigma\,\vartheta(x)$ with $\varsigma \neq 0$ is any representative of the same projective charge class, then, with respect to the tangential–normal splitting $\mathbb{R}^3 = \vec{P} \oplus \vec{P}^{\perp}$, the full Hessian of V_q at x is $\varsigma H_0(x) \oplus (-\varsigma)$.

The charge-variation map

$$K_x : \mathbb{R}^3 \longrightarrow \vec{P}, \qquad K_x(\dot{q}) = -\sum_i \frac{\dot{q}_i}{r_i^3} u_i,$$

has kernel $\mathbb{R}\vartheta(x)$ and induces an isomorphism $\overline{K}_x : \mathbb{R}^3/\mathbb{R}\vartheta(x) \to \vec{P}$. Evaluation at $\vartheta(x)$ identifies

$$T_{\Theta(x)}\mathbb{RP}^2 \cong \operatorname{Hom}\Big(\mathbb{R}\vartheta(x), \mathbb{R}^3/\mathbb{R}\vartheta(x)\Big) \cong \mathbb{R}^3/\mathbb{R}\vartheta(x).$$

Under this identification,

$$H_0(x) + \overline{K}_x\, d\Theta_x = 0, \qquad d\Theta_x = -\overline{K}_x^{-1} H_0(x), \tag{2.3}$$

and consequently

$$\operatorname{rank} d\Theta_x < 2 \quad \Longleftrightarrow \quad |\Xi(x)| = 1/3, \tag{2.4}$$

with $d\Theta_x$ of rank one on this level.

Finally, for such q, the equilibrium x is nondegenerate and has local Brouwer index $+1$ for $\nabla_P V_q$ when $|\Xi(x)| < 1/3$; it is a regular saddle of index -1 when $|\Xi(x)| > 1/3$; and it is corank-one degenerate when $|\Xi(x)| = 1/3$.

Proof. For a single source, $\nabla_P^2(|u|^{-1}) = (3uu^{\mathsf{T}} - |u|^2 I)/|u|^5$ on $\vec{P}$. Hence, with $q_i = \lambda_i r_i^3$,

$$H_0 = \sum_i \lambda_i \Big(3\frac{u_i u_i^{\mathsf{T}}}{r_i^2} - I\Big) = 3\sum_i \lambda_i \widehat{u}_i \widehat{u}_i^{\mathsf{T}} - I, \qquad \widehat{u}_i = u_i/r_i.$$

For a unit vector at angle α one has $\widehat{u}\widehat{u}^{\mathsf{T}} = \frac{1}{2}(I + \mathsf{M}(e^{2i\alpha}))$, so $H_0 = \frac{3}{2}I + \frac{3}{2}\mathsf{M}(\Xi) - I$, which is (2.2). The matrix $\mathsf{M}(z)$ is symmetric and traceless with eigenvalues $\pm|z|$, so H_0 has eigenvalues $(1 \pm 3|\Xi|)/2$ and unit trace. Since V_q is harmonic and the mixed derivatives vanish on P by reflection symmetry, the normal second derivative equals $-\varsigma$, which gives the stated block form.

The planar eigenvalues of the scaled Hessian are $\varsigma(1 \pm 3|\Xi|)/2$, and therefore

$$\det(\varsigma H_0) = \frac{\varsigma^2}{4}(1 - 9|\Xi|^2).$$

This proves the three index and degeneracy assertions in the statement.

The map K_x is exactly $\dot{q} \mapsto \nabla_P V_{\dot{q}}(x)$; by the proof of Lemma 2.2 its kernel is $\mathbb{R}\vartheta(x)$, so it induces an isomorphism $\overline{K}_x : \mathbb{R}^3/\mathbb{R}\vartheta(x) \to \vec{P}$. In the standard projective tangent-space model displayed in the statement, evaluation at the chosen representative $\vartheta(x)$ sends $d\Theta_x(v)$ to the class $[d\vartheta_x(v)]$.

The incidence equation $\nabla_P V_{\vartheta(x)}(x) = -\sum_i \lambda_i u_i = 0$ holds identically in x. Differentiating in a direction $v \in \vec{P}$, with the charge held fixed in the spatial derivative, gives $H_0(x)v + K_x(d\vartheta_x(v)) = 0$. Since $K_x(d\vartheta_x(v)) = \overline{K}_x(d\Theta_x(v))$, this is (2.3). The isomorphism $\overline{K}_x$ gives $\operatorname{rank} d\Theta_x = \operatorname{rank} H_0(x)$, while $\det H_0 = (1 - 9|\Xi|^2)/4$. This proves (2.4); on the stated level H_0 has eigenvalues 0 and 1, so the rank is one. □

A signed Jacobian of Θ will only be used after choosing an oriented affine chart in a fixed projective charge orthant, where the coordinate signs are fixed modulo simultaneous reversal. No global orientation of $\mathbb{RP}^2$ is assumed.

Lemma 2.4 (Localization)**.** *Let O and R_c be the circumcenter and circumradius of T. Then*

$$1 - |\Xi|^2 = \frac{16S^2\lambda_1\lambda_2\lambda_3(R_c^2 - |x - O|^2)}{r_1^2 r_2^2 r_3^2}. \tag{2.5}$$

Consequently $\overline{\mathcal{R}}$ can meet only four barycentric sign chambers, namely $(+++)$, which is $\operatorname{int} T$*, and the three chambers with a single negative coordinate; we call these four chambers* admissible*. In each one-negative chamber, $\overline{\mathcal{R}}$ lies outside the circumcircle. Moreover, if $\Theta(x) = \Theta(x')$ with $x, x' \in \overline{\mathcal{R}}$, then x and x' lie in the same strict barycentric sign chamber.*

Proof. Since $|e_i| = 1$ and $\sum_i \lambda_i = 1$, expanding both sides gives the elementary identity $1 - \left|\sum_i \lambda_i e_i\right|^2 = \sum_{i<j} \lambda_i\lambda_j |e_i - e_j|^2$. Next, $e_i - e_j = (u_i\bar{u}_j - u_j\bar{u}_i)/(\bar{u}_i\bar{u}_j)$ and if ε_{ijk} denotes the alternating symbol with $\varepsilon_{123} = 1$, then $\det(u_i, u_j) = 2S\varepsilon_{ijk}\lambda_k$ and $\Im(u_i\bar{u}_j) = -2S\varepsilon_{ijk}\lambda_k$. Hence, for $\{i, j, k\} = \{1, 2, 3\}$,

$$|e_i - e_j|^2 = \frac{16S^2\lambda_k^2}{r_i^2 r_j^2}$$

and therefore

$$1 - |\Xi|^2 = \frac{16S^2\lambda_1\lambda_2\lambda_3}{r_1^2 r_2^2 r_3^2} \sum_k \lambda_k r_k^2.$$

Finally, since $|a_i - O| = R_c$ and $\sum_i \lambda_i(a_i - O) = x - O$,

$$\sum_i \lambda_i r_i^2 = |x - O|^2 - 2\left\langle x - O, \sum_i \lambda_i(a_i - O)\right\rangle + R_c^2 = R_c^2 - |x - O|^2.$$

Combining these identities gives (2.5).

No point of $\overline{\mathcal{R}}$ has a vanishing barycentric coordinate: on $L_{ij} \setminus \{a_i, a_j\}$, where $L_{ij} = \operatorname{aff}\{a_i, a_j\}$, one has $\lambda_k = 0$ and $e_i = e_j$, hence $|\Xi| = 1$. No point of $\overline{\mathcal{R}}$ lies in a chamber with two negative coordinates: if $\lambda_i > 0 > \lambda_j, \lambda_k$ then the reverse triangle inequality gives

$$|\Xi| \geq \lambda_i - |\lambda_j| - |\lambda_k| = \lambda_i + \lambda_j + \lambda_k = 1.$$

The pattern $(---)$ is impossible because $\sum_i \lambda_i = 1$. This leaves the four possible chambers, and (2.5) together with $1 - |\Xi|^2 > 0$ forces $|x - O| > R_c$ in each one-negative chamber.

For the last statement, $\Theta(x) = \Theta(x')$ means $\lambda_i(x) r_i(x)^3 = \varsigma\, \lambda_i(x') r_i(x')^3$ for all i and some $\varsigma \neq 0$, so the two sign patterns are equal or opposite. None of the four admissible patterns is the negative of another, so they are equal. $\square$

Section 3 shows that the portion of $\overline{\mathcal{R}}$ in each admissible chamber is a closed disc.

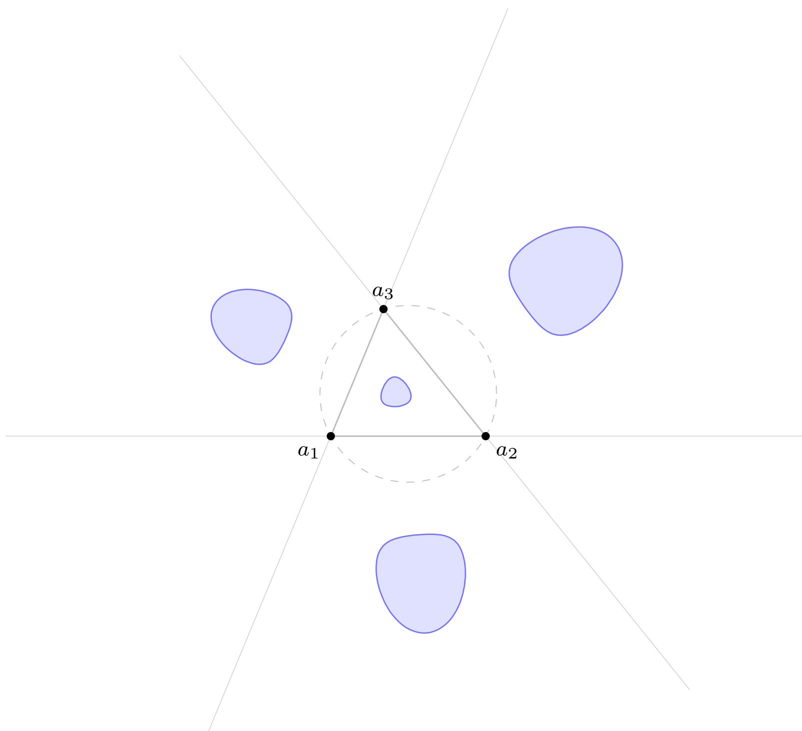

Figure 1: A numerical plot of the region $\mathcal{R} = \{|\Xi| < 1/3\}$ for the triangle $a_1 = 0$, $a_2 = 1$, $a_3 = 0.34 + 0.82\, i$. It consists of four open discs, one in each admissible barycentric sign chamber: the chamber $(+\,+\,+)$ inside the triangle, and the three chambers with a single negative coordinate, which lie across the corresponding side and, by Lemma 2.4, outside the circumcircle (dashed). The site lines are shown in grey.

3 The four elliptic discs

After applying the orientation-preserving similarity $z \mapsto (z - a_1)/(a_2 - a_1)$, we use the normalization

$$a_1 = 0, \qquad a_2 = 1, \qquad a_3 = \xi_0 + i\eta_0, \qquad \eta_0 > 0. \tag{3.1}$$

Here $2S = \eta_0 > 0$ and the complex orientation of the x-plane is the chosen one. The change of coordinates multiplies Ξ by a fixed unit complex number, so it preserves $|\Xi|$, the sign of $\operatorname{Jac} \Xi$, and all winding numbers. We write $L_1 = |a_2 - a_3|^2$, $L_2 = |a_3 - a_1|^2$, $L_3 = |a_1 - a_2|^2$ and $\ell_i = \sqrt{L_i}$, and we let φ_i be the interior angle of T at a_i. Unless a compactification is explicitly named, closures and boundaries in this section are taken relative to P_A.

3.1 Boundary behaviour of Ξ

We first record, once and for all, the compactification used for both chamber types. Let $\mathcal{S}_0$ be a compact set of normalized shapes (ξ_0, η_0) in the open upper half-plane.

Lemma 3.1 (Boundary behaviour)**.** *Uniformly for $(\xi_0, \eta_0) \in \mathcal{S}_0$:*

(i) *On an open side $\lambda_i = 0$ one has $\Xi = e_j = e_k$; this value is constant along the side and has modulus one.*

(ii) *If $x - a_i = re^{i\theta}$ with $r \to 0$, then $\Xi = e^{2i\theta} + O(r)$, uniformly in θ.*

(iii) *As $|x| \to \infty$, $\Xi(x) = x/\bar{x} + O(|x|^{-1})$, uniformly in $\arg x$.*

After identifying the chambers by the fixed barycentric charts used below, Ξ extends jointly continuously in $(\xi_0, \eta_0) \in \mathcal{S}_0$ to a fixed compactified chamber. In the interior case this compactification real-blows up the three vertices of the closed triangle; in the edge case it real-blows up the two finite site corners and adjoins the boundary arc at infinity. On every boundary face one has $|\Xi| = 1$. Consequently, for every $\epsilon > 0$, the set of pairs consisting of a shape in $\mathcal{S}_0$ and a point in its open chamber at which $|\Xi| \le 1 - \epsilon$ is compact in the product of $\mathcal{S}_0$ with the fixed chamber chart.

Proof. (i) If $\lambda_i = 0$ then $\lambda_j u_j + \lambda_k u_k = 0$ with $\lambda_j + \lambda_k = 1$, so u_j and u_k are parallel. Since $u \mapsto u/\bar{u}$ is invariant under multiplication of u by a nonzero real, $e_j = e_k$ and $\Xi = \lambda_j e_j + \lambda_k e_k = e_j$. Along the side $a_j a_k$ the direction of u_j is constant, so Ξ is constant of modulus one.

(ii) Cramer's rule gives $\lambda_j, \lambda_k = O(r)$ with constants bounded in terms of $1/\eta_0$ and $\max_{p,q} |a_p - a_q|$, hence uniformly on $\mathcal{S}_0$, while $\lambda_i \to 1$ and $|e_p| = 1$. Therefore $\Xi = e_i + O(r) = e^{2i\theta} + O(r)$.

(iii) Expanding,

$$e_i = \frac{x}{\bar{x}} + \frac{x\bar{a}_i - \bar{x}a_i}{\bar{x}^2} + O(|x|^{-2}).$$

Because $\sum_i \lambda_i = 1$ and $\sum_i \lambda_i a_i = x$, the first-order terms cancel exactly after summation: $\sum_i \lambda_i (x\bar{a}_i - \bar{x}a_i)/\bar{x}^2 = (x\bar{x} - \bar{x}x)/\bar{x}^2 = 0$. Since $\lambda_i = O(|x|)$ with constants uniform on $\mathcal{S}_0$, the remaining terms contribute $O(|x|^{-1})$.

For the compactification statement, consider the edge chamber; the interior chamber is the same argument with no face at infinity. In the chart of Section 3.3, start with the closed square $[0,1]^2$: the sides $s = 0$ and $s = 1$ are the two open sides of the chamber, the side $t = 0$ is the segment $a_2 a_3$, the corners $(0,0)$ and $(1,0)$ correspond to the sites a_3 and a_2, and $t = 1$ is the arc at infinity. Real-blow up the two site corners. Near either one the chart is an orientation-preserving diffeomorphism onto a sector at that site, so this blow-up matches the real blow-up of P at the site, and Ξ extends by (ii). On the face $t = 1$ the limit is $x/\bar{x}$ by (iii), with $\arg x$ the direction of the chamber ray determined by s; this depends continuously on s. At the two remaining corners $(0,1)$ and $(1,1)$ the two one-sided limits agree, because the chamber ray in direction $s \to 0$ is the ray of L_{13} beyond a_3 and that in direction $s \to 1$ is the ray of L_{12} beyond a_2, whose squared directions are precisely the constant values of Ξ on the sides $s = 0$ and $s = 1$ given by (i). All the estimates above are uniform on $\mathcal{S}_0$, so Ξ is jointly continuous on the compact product of the fixed compactified chamber with $\mathcal{S}_0$, with modulus one on every boundary face. A uniform boundary neighbourhood therefore satisfies $|\Xi| > 1 - \epsilon$. The sublevel set in the statement is a closed subset of the compact complement of this neighbourhood and is therefore compact. $\square$

3.2 Interior chamber

We first construct the polynomial that controls the Jacobian. Introduce an independent variable w, which on the real locus is set equal to $\bar{z}$, and put, for cyclic (i,j,k),

$$u_i = z - a_i, \qquad v_i = w - \bar{a}_i, \qquad D_i = v_j u_k - u_j v_k, \qquad c_i = a_k - a_j.$$

Then $\sum_i D_i = 2i\eta_0$. The rational functions $D_i/(2i\eta_0)$ are the complexifications of the barycentric coordinates: on the real locus $w = \bar{z}$ they equal λ_i. Thus $\sum_i D_i u_i/(2i\eta_0 v_i)$ restricts to Ξ, and exact differentiation of this complexification, followed by restriction to the real locus, gives

$$\Xi_z = \frac{\Pi}{2i\eta_0(v_1v_2v_3)^2}, \qquad \Xi_{\bar{z}} = \frac{\Pi^\sharp}{2i\eta_0(v_1v_2v_3)^2},$$

$$\Pi = \sum_{\text{cyc}} (\bar{c}_i u_i + D_i) v_i v_j^2 v_k^2, \qquad \Pi^\sharp = -\sum_{\text{cyc}} u_i (c_i v_i + D_i) v_j^2 v_k^2.$$

On the real locus, $\operatorname{Jac}\Xi = |\Xi_z|^2 - |\Xi_{\bar{z}}|^2$ and $|v_i| = r_i$. The difference $|\Pi^\sharp|^2 - |\Pi|^2$, expressed in the barycentric variables, is exactly divisible by $\lambda_1\lambda_2\lambda_3\eta_0^4$, and we *define*

$$|\Pi^\sharp|^2 - |\Pi|^2 = \lambda_1\lambda_2\lambda_3\,\eta_0^4\,\mathcal{V}. \tag{3.2}$$

Then

$$\operatorname{Jac}\Xi = \frac{|\Pi|^2 - |\Pi^\sharp|^2}{4\eta_0^2\, r_1^4 r_2^4 r_3^4} = -\frac{S^2\lambda_1\lambda_2\lambda_3}{r_1^4 r_2^4 r_3^4}\,\mathcal{V}. \tag{3.3}$$

As constructed, $\mathcal{V}$ is a polynomial in $(\lambda_1,\lambda_2,\lambda_3)$, homogeneous of degree 11, whose coefficients are polynomials in ξ_0, η_0 involving only even powers of η_0. Substituting $\eta_0^2 = L_2 - \xi_0^2$ and $\xi_0 = (1+L_2-L_1)/2$, and then homogenizing with L_3 (which equals 1 in the normalization (3.1)), expresses $\mathcal{V}$ as a polynomial

$$\mathcal{V} = \mathcal{V}(\lambda_1,\lambda_2,\lambda_3; L_1, L_2, L_3),$$

bihomogeneous of degree 11 in the λ_i and degree 3 in the L_i, and invariant under every simultaneous permutation of the paired variables (λ_i, L_i). All of this is verified exactly in `certificates/interior_jacobian.py`; see Appendix A.

Under a similarity of length scale ρ, the factors S^2, $r_1^4r_2^4r_3^4$, and $\mathcal{V}$ in (3.3) scale as ρ^4, ρ^{12}, and ρ^6, respectively. Thus both sides of (3.3) scale as ρ^{-2}; in particular, the sign of $\operatorname{Jac}\Xi$ is similarity invariant.

Proposition 3.2 (Interior disc)**.** $\operatorname{Jac}\Xi < 0$ *throughout* $\operatorname{int} T$*, the map* $\Xi : \operatorname{int} T \to \mathbb{D} = \{|z| < 1\}$ *is an orientation-reversing diffeomorphism, and* $\Xi^{-1}\{|z| \le 1/3\}$ *is a closed disc contained in* $\operatorname{int} T$ *whose boundary* $\Xi^{-1}\{|z| = 1/3\}$ *is one smooth circle.*

Proof. Put $y_i = (\ell_j + \ell_k - \ell_i)/2$, which is positive by the strict triangle inequality, and apply the Ravi substitution $L_i = (y_j + y_k)^2$. With $X = (\lambda_1,\lambda_2,\lambda_3,y_1,y_2,y_3)$ the resulting polynomial $\mathcal{V}_{\text{Ravi}}$ is bihomogeneous of degree $(11,6)$ with integer coefficients, and it admits the exact decomposition

$$\mathcal{V}_{\text{Ravi}} = \sum_{r=1}^{30} \frac{\mathsf{n}_r}{2}\left(X^{\alpha_r} + X^{\gamma_r} - 2X^{\beta_r}\right) + \mathcal{T}(X), \qquad \alpha_r + \gamma_r = 2\beta_r, \tag{3.4}$$

where $\mathsf{n}_r \in \mathbb{Z}_{>0}$, $\alpha_r, \beta_r, \gamma_r \in \mathbb{Z}^6_{\geq 0}$, and $X^\alpha = \prod_{j=1}^6 X_j^{\alpha_j}$. The thirty quadruples $(\mathsf{n}_r, \alpha_r, \gamma_r, \beta_r)$ are listed in Table 1; the monomials X^{β_r} are precisely the thirty monomials of $\mathcal{V}_{\text{Ravi}}$ with a negative coefficient. Each bracketed expression in (3.4) is nonnegative for $X > 0$ by the AM–GM inequality, because $\alpha_r + \gamma_r = 2\beta_r$. The remainder $\mathcal{T}$ has 1548 terms, all of its coefficients are positive integers, and the smallest of them is 16; in particular $\mathcal{T}(X) > 0$ for $X > 0$. Hence $\mathcal{V}_{\text{Ravi}} > 0$ for positive X, so $\mathcal{V} > 0$ for positive barycentrics, and (3.3) gives $\operatorname{Jac}\Xi < 0$ on $\operatorname{int} T$.

The circumdisc is convex and contains the three vertices, so every point of $\operatorname{int} T$ lies strictly inside it. Hence (2.5) gives $|\Xi| < 1$ there. By Lemma 3.1, Ξ extends continuously to the compact surface $\widehat{T}$ obtained by blowing up the three vertices, with modulus one on $\partial\widehat{T}$. For every compact $K \Subset \mathbb{D}$ the set $\Xi^{-1}(K)$ is closed in $\widehat{T}$ and disjoint from $\partial\widehat{T}$, hence compact in $\operatorname{int} T$; therefore

$$\Xi : \operatorname{int} T \longrightarrow \mathbb{D}$$

is proper. For $y \in \mathbb{D}$, the boundary formula for Brouwer degree gives

$$\deg(\Xi, \operatorname{int} T, y) = \operatorname{wind}_{\partial\widehat{T}}(\Xi - y).$$

Since $|\Xi| = 1 > |y|$ on $\partial\widehat{T}$, the homotopy $\Xi - ty$, $0 \leq t \leq 1$, never vanishes there. Thus this winding equals the degree of the boundary map $\Xi|_{\partial\widehat{T}} : \partial\widehat{T} \to S^1$. By Lemma 3.1(i), the side pieces of $\partial\widehat{T}$ map to constants. Traversing $\partial\widehat{T}$ positively, one enters the blow-up arc at a_i along one side and leaves along the other, so $\arg u_i$ decreases by the interior angle φ_i and $\arg\Xi$ decreases by $2\varphi_i$. Thus the boundary degree is $-2(\varphi_1 + \varphi_2 + \varphi_3)/(2\pi) = -1$.

Properness and local nonsingularity make every fibre finite. Since every local Jacobian is negative, for every $y \in \mathbb{D}$

$$-1 = \deg(\Xi, \operatorname{int} T, y) = -\#\Xi^{-1}(y),$$

so Ξ is a bijection onto $\mathbb{D}$; being also a local diffeomorphism, it is a diffeomorphism. It restricts to a diffeomorphism from $\Xi^{-1}\{|z| \leq 1/3\}$ onto the closed disc $\{|z| \leq 1/3\}$; hence this preimage is a smoothly embedded closed disc whose boundary is the smooth circle $\Xi^{-1}\{|z| = 1/3\}$. ☐

3.3 Edge chambers

By the cyclic relabelling fixed in Section 1.1 it is enough to consider $\lambda_1 < 0 < \lambda_2, \lambda_3$. Use the homogeneous barycentric coordinates

$$(\hat\lambda_1 : \hat\lambda_2 : \hat\lambda_3) = (-t : s : 1 - s), \qquad 0 < s, t < 1;$$

the normalized coordinates are $(-t, s, 1-s)/(1-t)$. Conversely, for normalized barycentrics with $\lambda_1 < 0 < \lambda_2, \lambda_3$, set

$$s = \frac{\lambda_2}{\lambda_2 + \lambda_3}, \qquad t = \frac{-\lambda_1}{\lambda_2 + \lambda_3}.$$

Then $0 < s, t < 1$, $\lambda = (-t, s, 1-s)/(1-t)$, and

$$\det \frac{\partial(\lambda_2, \lambda_3)}{\partial(s, t)} = (1-t)^{-3} > 0.$$

Since $S > 0$, the affine chart $(\lambda_2, \lambda_3) \mapsto x$ is orientation preserving; hence so is (s, t), which is therefore a global orientation-preserving chart of the strict edge chamber. Although $L_3 = \ell_3 = 1$ in (3.1), we retain these variables below to display the homogeneous formulas. Put

$$K_{\mathrm{e}} = L_1 s(1-s), \qquad D_{\mathrm{e}} = L_2(1-s) + L_3 s, \qquad P_{\mathrm{e}} = D_{\mathrm{e}} t - K_{\mathrm{e}},$$

and, with $(\hat\lambda_1, \hat\lambda_2, \hat\lambda_3) = (-t, s, 1-s)$,

$$\begin{aligned}
\mathcal{Q}_1 &= L_3\hat\lambda_2^2 + (L_2 + L_3 - L_1)\hat\lambda_2\hat\lambda_3 + L_2\hat\lambda_3^2,\\
\mathcal{Q}_2 &= L_1\hat\lambda_3^2 + (L_3 + L_1 - L_2)\hat\lambda_3\hat\lambda_1 + L_3\hat\lambda_1^2,\\
\mathcal{Q}_3 &= L_2\hat\lambda_1^2 + (L_1 + L_2 - L_3)\hat\lambda_1\hat\lambda_2 + L_1\hat\lambda_2^2.
\end{aligned}$$

Expanding $x - a_i$ in the two edge vectors at a_i gives $\mathcal{Q}_i = (\hat\lambda_1 + \hat\lambda_2 + \hat\lambda_3)^2 r_i^2 > 0$. Writing $\mathcal{H} = 1 - |\Xi|^2$ and using Heron's formula $2L_1L_2 + 2L_1L_3 + 2L_2L_3 - L_1^2 - L_2^2 - L_3^2 = 16S^2$, direct substitution in (2.5) gives

$$\mathcal{H} = \frac{\Phi}{\mathcal{Q}}, \qquad \Phi = 16S^2\, ts(1-s)P_{\mathrm{e}}(1-t), \qquad \mathcal{Q} = \mathcal{Q}_1\mathcal{Q}_2\mathcal{Q}_3, \tag{3.5}$$

the key intermediate identity being $\hat\lambda_1\mathcal{Q}_1 + \hat\lambda_2\mathcal{Q}_2 + \hat\lambda_3\mathcal{Q}_3 = -(1-t)P_{\mathrm{e}}$. Thus the fold equation is

$$\mathcal{L} := 9\Phi - 8\mathcal{Q} = 0. \tag{3.6}$$

On the fold $\{\mathcal{L} = 0\}$ one has $\mathcal{H} = 8/9 > 0$, so (3.5) gives $\Phi > 0$ and therefore $P_{\mathrm{e}} > 0$.

Proposition 3.3 (Edge fold is regular)**.** *In every edge chamber,*

$$|\Xi| = 1/3 \quad\Longrightarrow\quad d|\Xi|^2 \neq 0. \tag{3.7}$$

Proof. On the fold (3.6) we have $\mathcal{H} = \Phi/\mathcal{Q}$ with $9\Phi = 8\mathcal{Q}$, so for $j \in \{s, t\}$

$$\mathcal{H}_j = \frac{\Phi_j\mathcal{Q} - \Phi\mathcal{Q}_j}{\mathcal{Q}^2} = \frac{9\Phi_j - 8\mathcal{Q}_j}{9\mathcal{Q}} = \frac{\Phi\,\mathcal{L}_j}{8\mathcal{Q}^2} \qquad \text{on } \{\mathcal{L} = 0\}.$$

The numerator $\Phi_t\mathcal{Q} - \Phi\mathcal{Q}_t$ of $\mathcal{H}_t$ factors exactly, as an identity of polynomials, as

$$\Phi_t\mathcal{Q} - \Phi\mathcal{Q}_t = -16S^2 s(1-s)\,\mathcal{Q}_1\mathcal{G}_1\mathcal{G}_2, \tag{3.8}$$

$$\mathcal{G}_1 = K_{\mathrm{e}}(1-2t) + D_{\mathrm{e}}t^2, \qquad \mathcal{G}_2 = P_{\mathrm{e}}^2 - \ell_2^2\ell_3^2 t^2(1-t)^2.$$

If $\mathcal{G}_1 = 0$ then $D_{\mathrm{e}}t^2 = K_{\mathrm{e}}(2t-1)$ forces $t > 1/2$, whence $P_{\mathrm{e}} = K_{\mathrm{e}}(t-1)/t < 0$, a contradiction. Moreover

$$\mathcal{G}_2 = \mathcal{G}_0\big(P_{\mathrm{e}} + \ell_2\ell_3 t(1-t)\big), \qquad \mathcal{G}_0 := P_{\mathrm{e}} - \ell_2\ell_3 t(1-t),$$

and the second factor is positive. Hence, at a fold point with $d\mathcal{H} = 0$, we get $\mathcal{G}_0 = 0$ from $\mathcal{H}_t = 0$ and $\mathcal{L}_s = 0$ from $\mathcal{H}_s = 0$, so that

$$\mathcal{L} = \mathcal{L}_s = \mathcal{G}_0 = 0.$$

We eliminate t. In the strict chamber the leading coefficients in t do not vanish:

$$\mathrm{lc}_t\,\mathcal{L} = -8\ell_2^2\ell_3^2\,\mathcal{Q}_1, \qquad \mathrm{lc}_t\,\mathcal{G}_0 = \ell_2\ell_3,$$

so the resultant computed over $\mathbb{Q}(\ell_1, \ell_2, \ell_3, s)[t]$ specializes faithfully. Exact elimination gives

$$\mathrm{Res}_t(\mathcal{L},\mathcal{G}_0) = s^2(1-s)^2\ell_1^4\ell_2^2\ell_3^2(\ell_1-\ell_2+\ell_3)^2(\ell_1+\ell_2-\ell_3)^2\mathcal{Q}_1^2\,\mathcal{E}^2, \tag{3.9}$$

where

$$\begin{aligned}\mathcal{E} = \ell_1^2 s^2 - \ell_1^2 s - 9\ell_2^2 s^2 + 17\ell_2^2 s - 8\ell_2^2 \\ - 18\ell_2\ell_3 s^2 + 18\ell_2\ell_3 s - 9\ell_3^2 s^2 + \ell_3^2 s.\end{aligned}$$

Next, $\mathrm{Res}_t(\mathcal{L}_s,\mathcal{G}_0)$ is exactly divisible by $s(s-1)\ell_1^4\ell_2\ell_3(\ell_1-\ell_2+\ell_3)^2(\ell_1+\ell_2-\ell_3)^2\mathcal{Q}_1$, and we define $\mathcal{S}\in\mathbb{Z}[\ell_1,\ell_2,\ell_3,s]$ by the exact quotient

$$\mathrm{Res}_t(\mathcal{L}_s,\mathcal{G}_0) = s(s-1)\ell_1^4\ell_2\ell_3(\ell_1-\ell_2+\ell_3)^2(\ell_1+\ell_2-\ell_3)^2\mathcal{Q}_1\,\mathcal{S}. \tag{3.10}$$

The quotient has zero remainder, so this specifies $\mathcal{S}$ uniquely; as an element of $\mathbb{Z}[\ell_1,\ell_2,\ell_3][s]$ it has degree 6 in s, it has total degree 14, and it is displayed in Appendix B. For (3.10) we use only the elementary implication that two polynomials with a common root have singular Sylvester matrix, whatever formal degrees are used; no hypothesis on $\mathrm{lc}_t\,\mathcal{L}_s$ is needed.

All displayed factors other than $\mathcal{E}$ and $\mathcal{S}$ are nonzero in the strict chamber, so $\mathcal{L}=\mathcal{L}_s=\mathcal{G}_0=0$ forces $\mathcal{E}=\mathcal{S}=0$ at the same value of s. Eliminating s gives

$$\begin{aligned}\mathrm{Res}_s(\mathcal{E},\mathcal{S}) = 5184\,\ell_2^6\ell_3^6(\ell_1-3\ell_2-3\ell_3)^2(\ell_1-\ell_2-\ell_3)^4(\ell_1+\ell_2+\ell_3)^4 \\ \cdot(\ell_1+3\ell_2+3\ell_3)^2(\ell_1^2-\ell_2^2-34\ell_2\ell_3-\ell_3^2)^2.\end{aligned} \tag{3.11}$$

Every factor is nonzero for a nondegenerate triangle. For example, $\ell_1<\ell_2+\ell_3$ implies

$$\ell_1^2-\ell_2^2-34\ell_2\ell_3-\ell_3^2 < (\ell_2+\ell_3)^2-\ell_2^2-34\ell_2\ell_3-\ell_3^2 = -32\ell_2\ell_3 < 0;$$

the remaining assertions follow immediately from the strict triangle inequalities. Hence $\mathcal{E}$ and $\mathcal{S}$ have no common root, a contradiction, which proves (3.7). The polynomials $\mathcal{E},\mathcal{S},\mathcal{Q}_i$, the factorization (3.8) and all three resultants are reconstructed in `certificates/edge_fold.py`. $\square$

Proposition 3.4 (Edge disc)**.** *For every nondegenerate triangle and every edge chamber, the set $\{\mathcal{H}\geq 8/9\}$ is a closed disc contained in the open chamber, and $\{\mathcal{H}=8/9\}$ is its single boundary circle.*

Proof. We first anchor the topology at the equilateral triangle. Put $\mathcal{K}_t=\Phi_t\mathcal{Q}-\Phi\mathcal{Q}_t$ and $\mathcal{K}_s=\Phi_s\mathcal{Q}-\Phi\mathcal{Q}_s$ after setting $\ell_1=\ell_2=\ell_3=1$; a critical point of $\mathcal{H}$ is exactly a common zero of $\mathcal{K}_s$ and $\mathcal{K}_t$. The complete elimination, rather than a selected-factor check, is

$$\begin{aligned}\mathrm{Res}_t(\mathcal{K}_t,\mathcal{K}_s) = -3^{15}s^{19}(s-1)^{19}(2s-1)^6(s^2-s+1)^{19} \\ \cdot(2s^2-2s-1)^2(2s^2-2s+1)^2.\end{aligned}$$

For $0<s<1$ this forces $s=1/2$; substitution gives exactly two critical points in the open square $(0,1)^2$, namely

$$t=\frac{1}{2},\qquad t=1-\frac{\sqrt{3}}{2},$$

with $\mathcal{H}$-values 1 and $-1/3$ respectively. The first is the excenter $(s,t)=(1/2,1/2)$, at which

$$\mathcal{H}=1,\qquad \mathrm{Hess}_{(s,t)}\,\mathcal{H}=\mathrm{diag}(-32/3,-32)$$

in the ordered coordinates (s,t). Since $\mathcal{H} = 1 - |\Xi|^2 \le 1$ everywhere, the excenter is the unique global maximum, and it is the only critical point with $\mathcal{H} \ge 8/9$.

By Lemma 3.1, $\mathcal{H} \to 0$ at every compactified end of the chamber, so $\{\mathcal{H} \ge 8/9\}$ is compact and contained in the open chamber. Choose a Morse neighbourhood U of the excenter in the compactified chamber $\widehat{C}$. Since the excenter is the unique point at which $\mathcal{H} = 1$, compactness gives

$$c_U := \max_{\widehat{C}\setminus U} \mathcal{H} < 1.$$

For a sufficiently small $0 < \varepsilon < \min\{1/9, 1 - c_U\}$, the entire set $\{\mathcal{H} \ge 1 - \varepsilon\}$ lies in U, and the Morse lemma identifies it with a single closed disc. The band $\{8/9 \le \mathcal{H} \le 1 - \varepsilon\}$ is compact and contains no critical point. Hence the vector field

$$\mathcal{X} = -\frac{\nabla \mathcal{H}}{\|\nabla \mathcal{H}\|^2}, \qquad d\mathcal{H}(\mathcal{X}) = -1,$$

is defined on an open neighbourhood of the band after that neighbourhood is chosen to contain no critical point. Compactness of the band then ensures that its flow exists for the finite time $1 - \varepsilon - 8/9$. It carries $\{\mathcal{H} = 1 - \varepsilon\}$ diffeomorphically onto $\{\mathcal{H} = 8/9\}$ and exhibits $\{\mathcal{H} \ge 8/9\}$ as the union of $\{\mathcal{H} \ge 1 - \varepsilon\}$ with a collar. Therefore, for the equilateral triangle, $\{\mathcal{H} \ge 8/9\}$ is a closed disc with a single boundary circle.

To continue the *filled* disc to an arbitrary shape, join the equilateral shape to the given one by the smooth straight-line path $\tau \mapsto (\xi_0(\tau), \eta_0(\tau))$, $\tau \in [0,1]$, inside the open upper half-plane; its image $\mathcal{S}_0$ is compact. Use the fixed edge chart, write $x = (s,t) \in (0,1)^2$, and set

$$\mathcal{Z} = \{(\tau, x) \in [0,1] \times (0,1)^2 : \mathcal{H}_\tau(x) \ge 8/9\}.$$

The uniform compactness assertion of Lemma 3.1, applied with $\epsilon = 2/3$, shows that $\mathcal{Z}$ is compact. Write $\mathcal{Z}_\tau = \{x : (\tau, x) \in \mathcal{Z}\}$ and

$$\mathcal{M} = \partial_{\mathrm{lat}} \mathcal{Z} = \{(\tau, x) : \mathcal{H}_\tau(x) = 8/9\}.$$

Proposition 3.3 gives $d_x \mathcal{H}_\tau \ne 0$ on $\mathcal{M}$. Consequently $\mathcal{Z}$ is a compact manifold with corners whose lateral boundary is $\mathcal{M}$, and both the projection $\pi : \mathcal{Z} \to [0,1]$ and its restriction to $\mathcal{M}$ are proper submersions. On $\mathcal{M}$ the vector field

$$Y = \partial_\tau - \frac{\partial_\tau \mathcal{H}}{\|\nabla_x \mathcal{H}\|^2} \nabla_x \mathcal{H}$$

satisfies $d\pi(Y) = 1$ and $d\mathcal{H}(Y) = 0$; extend its spatial part to a collar neighbourhood of $\mathcal{M}$ in $\mathcal{Z}$, and then to all of $\mathcal{Z}$ by blending it with the zero spatial field away from that collar. Throughout this extension $d\pi(Y) = 1$, and Y remains tangent to the lateral boundary. Because $\mathcal{Z}$ is compact, each integral curve exists for every time for which its τ-coordinate remains in $[0,1]$. The time-τ map gives, equivalently to the boundary version of Ehresmann's fibration theorem [3, Ch. II, §1], diffeomorphisms of pairs

$$(\mathcal{Z}_0, \partial \mathcal{Z}_0) \cong (\mathcal{Z}_\tau, \partial \mathcal{Z}_\tau).$$

Thus the equilateral closed disc and its single boundary circle continue to every nondegenerate triangle. □

Proposition 3.5 (The four discs)**.** *$\mathcal{R}$ is the disjoint union of four open discs Ω, one in each admissible sign chamber; each $\overline{\Omega}$ is contained in the open chamber. Moreover,*

$$\overline{\mathcal{R}} = \{x \in P_A : |\Xi(x)| \le 1/3\} = \bigsqcup_{\Omega} \overline{\Omega}, \qquad \partial\mathcal{R} = \{x \in P_A : |\Xi(x)| = 1/3\} = \bigsqcup_{\Omega} \partial\Omega,$$

and every $\partial\Omega$ is a smooth Jordan curve on which $d|\Xi|^2 \neq 0$, and

$$\operatorname{wind}_{\partial\Omega} \Xi = -1 \tag{3.12}$$

for the positive boundary orientation.

Proof. The site-line identity $|\Xi| = 1$ and the reverse-triangle estimate $|\Xi| \ge 1$ in every two-negative chamber, proved in Lemma 2.4, show that the weak sublevel $\{|\Xi| \le 1/3\}$ meets only the four admissible chambers. Its trace on each is $\{\mathcal{H} \ge 8/9\}$, which is a closed disc by Proposition 3.2 in the interior chamber and by Proposition 3.4 in the edge chambers; in both cases its boundary is the level $|\Xi| = 1/3$. Its interior is therefore the strict sublevel $|\Xi| < 1/3$. This proves the asserted disc decomposition and both displayed set identities. Regularity of $d|\Xi|^2$ on the boundary holds by Proposition 3.3 in the edge chambers, and in the interior chamber because Ξ is a diffeomorphism there and $|\Xi| = 1/3 \neq 0$.

For (3.12) in the interior chamber, Ξ maps $\partial\Omega$ onto the circle $\{|z| = 1/3\}$ by an orientation-reversing diffeomorphism, so the winding is -1.

For an edge chamber, let $\widehat{C}$ be its compactification as in Lemma 3.1; it is a closed disc. Traverse $\partial\widehat{C}$ positively. Its straight side pieces contribute zero by Lemma 3.1(i). The interior angle of the chamber at a_2 is $\pi - \varphi_2$ and at a_3 is $\pi - \varphi_3$, and the blown-up arcs there are traversed so that $\arg u_i$ *decreases* by the interior angle, exactly as in Proposition 3.2. The chamber subtends the angle φ_1 at infinity, and the arc at infinity is traversed counterclockwise, so $\arg x$ *increases* by φ_1. Since $\Xi = e^{2i\arg(x-a_i)} + o(1)$ at a site and $\Xi = e^{2i\arg x} + o(1)$ at infinity, the total change of $\arg \Xi$ is

$$-2(\pi - \varphi_2) - 2(\pi - \varphi_3) + 2\varphi_1 = -2\pi,$$

using $\varphi_1 + \varphi_2 + \varphi_3 = \pi$. Hence $\operatorname{wind}_{\partial\widehat{C}} \Xi = -1$. Now $\mathcal{A} := \widehat{C} \setminus \Omega$ is a compact annulus on which $|\Xi| \ge 1/3$, so $\Xi : \mathcal{A} \to \mathbb{C}^{\times}$. If $\partial\Omega$ is given the positive boundary orientation of $\overline{\Omega}$, then the oriented boundary chain is $\partial\mathcal{A} = \partial\widehat{C} - \partial\Omega$. Therefore

$$0 = \operatorname{wind}_{\partial\mathcal{A}} \Xi = \operatorname{wind}_{\partial\widehat{C}} \Xi - \operatorname{wind}^{+}_{\partial\Omega} \Xi,$$

and hence $\operatorname{wind}^{+}_{\partial\Omega} \Xi = -1$. The other edge chambers follow by the cyclic relabelling fixed in Section 1.1, which preserves the plane orientation. $\square$

4 The caustic line family

For each of the four discs in Proposition 3.5, call $\partial\Omega$ a *fold circle* and call $\mathcal{C}_\Omega := \Theta(\partial\Omega) \subset \mathbb{RP}^2$ its *projective caustic*. Let $x = x(s)$ be a smooth local parametrization of a fold circle with $x_s \neq 0$. Since $|\Xi| = 1/3$ there, choose a smooth local phase lift ψ such that

$$3\Xi = e^{i\psi}, \qquad \beta_i = \alpha_i - \psi/2,$$

and define

$$n_i = \frac{\sin\beta_i}{r_i^2}, \qquad \widehat{n}_i = \frac{\cos\beta_i}{r_i^2}, \qquad \nu_i = \lambda_i r_i^3. \tag{4.1}$$

Equivalently $n_i = \Im(e^{-i\psi/2}u_i)/r_i^3$ and $\widehat{n}_i = \Re(e^{-i\psi/2}u_i)/r_i^3$, so no lift of an individual angle α_i is needed. Replacing ψ by $\psi + 2\pi$ reverses n and $\widehat{n}$ simultaneously. Thus the projective covector $[n]$ and the cross products $n \times \widehat{n}$ and $n \times n_s$ are independent of the chosen local lift.

Lemma 4.1 (Line family)**.** *Along the preceding local parametrization,*

$$\langle \nu, n\rangle = \langle \nu, \widehat{n}\rangle = 0, \qquad n \times \widehat{n} = -\frac{2S}{(r_1r_2r_3)^3}\,\nu,$$

and $\langle n, \nu_s\rangle = \langle n_s, \nu\rangle = 0$. Consequently $\Theta(x(s)) = [\nu(s)] = [n(s) \times n_s(s)]$ whenever $n \times n_s \neq 0$. Moreover, the projective line

$$L_s := \{[q] \in \mathbb{RP}^2 : \langle n(s), q\rangle = 0\}$$

is tangent to the parametrized caustic branch wherever $(\Theta \circ x)_s \neq 0$. Along any sequence of such immersed parameters converging to s_0, the tangent lines converge to L_{s_0}. In particular, if s_0 is an isolated singular parameter of the caustic branch, as at an ordinary cusp, then L_{s_0} is its unique limiting tangent.

Proof. Barycentric closure gives $\langle \nu, n\rangle = \Im\big(e^{-i\psi/2}\sum_i \lambda_i u_i\big) = 0$ and likewise for $\widehat{n}$ with $\Re$ in place of $\Im$. For the first component of the cross product,

$$\begin{aligned}(n \times \widehat{n})_1 = \frac{\sin(\beta_2 - \beta_3)}{r_2^2 r_3^2} &= \frac{r_2r_3\sin(\alpha_2 - \alpha_3)}{r_2^3 r_3^3}\\ &= -\frac{2S\lambda_1}{r_2^3r_3^3} = -\frac{2S}{(r_1r_2r_3)^3}\,\nu_1,\end{aligned}$$

because $r_2r_3\sin(\alpha_2 - \alpha_3) = -\det(u_2, u_3) = -2S\lambda_1$. The other two components follow cyclically. Since $S > 0$, every $r_i > 0$, and $\nu \neq 0$, this cross product never vanishes; hence $n, \widehat{n}$ form a basis of the plane $\nu^\perp$.

For the remaining identities, note first that $H_0 = \frac{1}{2}\big(I + \mathsf{M}(e^{i\psi})\big)$ on the fold, so $\ker H_0 = \mathbb{R}\, ie^{i\psi/2}$. Put $e_0 = ie^{i\psi/2}$. For any charge variation $\dot{q}$,

$$\langle e_0, K_x(\dot{q})\rangle_{\vec{P}} = -\sum_i \frac{\dot{q}_i}{r_i^3}\,\Re\big(\overline{ie^{i\psi/2}}\,u_i\big) = -\sum_i \frac{\dot{q}_i}{r_i^3}\,\Im\big(e^{-i\psi/2}u_i\big) = -\langle \dot{q}, n\rangle_{\mathbb{R}^3}, \tag{4.2}$$

Thus, under the Euclidean identifications, the pullback covector $K_x^* e_0$ is $-n$. Direct differentiation of the canonical incidence identity $\nabla_P V_{\nu(s)}(x(s)) = 0$ gives

$$H_0(x)\,x_s + K_x(\nu_s) = 0.$$

This is the representative form of (2.3): the class of ν_s represents $d\Theta_x(x_s)$ modulo $\mathbb{R}\nu$, and $K_x(\nu) = 0$. Pairing with e_0 and using that H_0 is symmetric with $H_0e_0 = 0$ gives $\langle e_0, K_x(\nu_s)\rangle_{\vec{P}} = 0$, hence $\langle n, \nu_s\rangle_{\mathbb{R}^3} = 0$ by (4.2). Differentiating $\langle n, \nu\rangle = 0$ then gives $\langle n_s, \nu\rangle = 0$.

Thus $n, n_s \in \nu^\perp$, a two-dimensional space, so $n \times n_s$ is parallel to ν whenever it is nonzero. This proves $[\nu] = [n \times n_s]$ whenever $n \times n_s \neq 0$. If $(\Theta \circ x)_s \neq 0$, then $\nu_s \notin \mathbb{R}\nu$, so ν and ν_s are linearly independent. Both belong to $n^\perp$, and therefore $n^\perp = \operatorname{span}\{\nu, \nu_s\}$. Projectivizing this plane gives both the tangent line to the parametrized branch $[\nu(s)]$ and L_s. Finally, n is smooth and nowhere zero, so $L_s = \mathbb{P}(n(s)^\perp)$ varies continuously. The tangent lines at immersed parameters approaching s_0 therefore converge to L_{s_0}, which proves the limiting-tangent assertion. $\square$

5 Exact Lami lemma

Every fold circle lies in a strict barycentric chamber, so $r_i > 0$ and $\lambda_i \neq 0$ throughout this section. Recall that a *regular parameter* on a fold circle means a parameter s with $x_s \neq 0$.

Proposition 5.1 (Lami regularity)**.** *For every smooth regular local parametrization $x = x(s)$ of a fold circle, there are uniquely determined smooth functions $\mathfrak{a}, \mathfrak{b}$ such that*

$$n_s = \mathfrak{a}n + \mathfrak{b}\widehat{n}, \qquad \mathfrak{b} \neq 0.$$

Consequently $n \times n_s \neq 0$ everywhere on the fold.

Proof. By Lemma 4.1 the vectors $n, \widehat{n}$ are a basis of the plane $\nu^\perp$, which contains n_s; so smooth $\mathfrak{a}, \mathfrak{b}$ exist uniquely and the whole content is $\mathfrak{b} \neq 0$. On an overlap of two phase lifts, the triple $(n, \widehat{n}, n_s)$ changes by one simultaneous sign, so these coefficients agree and patch independently of that choice. More explicitly,

$$\mathfrak{a} = \frac{(n_s \times \widehat{n}) \cdot (n \times \widehat{n})}{|n \times \widehat{n}|^2}, \qquad \mathfrak{b} = \frac{(n \times n_s) \cdot (n \times \widehat{n})}{|n \times \widehat{n}|^2};$$

these formulas also make smoothness and lift invariance transparent. Put

$$\omega = \psi_s, \qquad z_i = e^{-i\psi/2}(x - a_i) = r_i e^{i\beta_i}, \qquad t_i = \tan \beta_i.$$

Step 1: the finite tangent chart. Suppose first that $\cos \beta_i \neq 0$ for all i. On the fold $3\Xi = e^{i\psi}$, so $\sum_i \lambda_i e^{2i\beta_i} = e^{-i\psi}\Xi = 1/3$. Taking real and imaginary parts of this together with $\sum_i \lambda_i = 1$, and writing $\mu_i = \lambda_i/(1 + t_i^2)$, gives

$$\sum_i \mu_i = \frac{2}{3}, \qquad \sum_i \mu_i t_i = 0, \qquad \sum_i \mu_i t_i^2 = \frac{1}{3}. \tag{5.1}$$

The t_i are pairwise distinct: equality of two would make the corresponding u_i parallel, putting x on a site line, where $|\Xi| = 1$, contrary to the fold equation $|\Xi| = 1/3$. Let $\mathsf{e}_1, \mathsf{e}_2, \mathsf{e}_3$ denote the elementary symmetric functions of t_1, t_2, t_3. Since the Vandermonde matrix is invertible, the unique solution of (5.1), with $(m_0, m_1, m_2) = (2/3, 0, 1/3)$, is, for $\{i, j, k\} = \{1, 2, 3\}$,

$$\mu_i = \frac{m_2 - (t_j + t_k)m_1 + t_j t_k m_0}{(t_i - t_j)(t_i - t_k)} = \frac{1 + 2t_j t_k}{3(t_i - t_j)(t_i - t_k)}.$$

Thus

$$\mu_i = \frac{d_i}{3(t_i - t_j)(t_i - t_k)}, \qquad \lambda_i = \frac{(1 + t_i^2)d_i}{3(t_i - t_j)(t_i - t_k)}, \qquad d_i = 1 + 2t_j t_k. \tag{5.2}$$

Here $d_i \neq 0$ because $\lambda_i \neq 0$.

For the radial data define the signed quantities $\eta_i = r_i/\cos \beta_i$, so that $z_i = \eta_i/(1 - it_i)$. The real and imaginary parts of $\sum_i \lambda_i z_i = 0$ are $\sum_i \mu_i \eta_i = 0$ and $\sum_i \mu_i t_i \eta_i = 0$. Hence, with $w_i = \mu_i \eta_i$,

$$(w_1, w_2, w_3) = \varkappa\,(t_2 - t_3,\ t_3 - t_1,\ t_1 - t_2)$$

for some $\varkappa$. Every μ_i and η_i is nonzero in this chart, so $w \neq 0$ and hence $\varkappa \neq 0$. Thus $\eta_i = \varkappa(t_j - t_k)/\mu_i$ for cyclic (i, j, k). By (5.2),

$$\eta_i d_i = 3\varkappa(t_j - t_k)(t_i - t_j)(t_i - t_k) = 3\varkappa\Delta, \qquad \Delta = (t_1 - t_2)(t_1 - t_3)(t_2 - t_3) \neq 0,$$

the last expression being the same for all three cyclic choices. Thus $\eta_i d_i$ is one common nonzero real number $C = 3\varkappa\Delta$, and

$$z_i = \frac{C}{(1 - it_i)d_i}. \tag{5.3}$$

The common value $C = \eta_i d_i$ is a smooth nowhere-zero real function on the finite chart. Write $X = e^{-i\psi/2}x_s$, $X/C = p_{\mathrm{L}} + iq_{\mathrm{L}}$, and $\gamma = C_s/C$. The sites are fixed, so $z_{i,s} = X - i\omega z_i/2$, and comparing $z_{i,s}/z_i$ computed from (5.3) with $X/z_i - i\omega/2$ yields

$$\begin{aligned} t_{i,s} &= (1 + t_i^2)\{d_i(q_{\mathrm{L}} - p_{\mathrm{L}}t_i) - \omega/2\},\\ \frac{r_{i,s}}{r_i} &= d_i(p_{\mathrm{L}} + q_{\mathrm{L}}t_i),\\ \gamma - \frac{d_{i,s}}{d_i} - \frac{t_i t_{i,s}}{1 + t_i^2} &= d_i(p_{\mathrm{L}} + q_{\mathrm{L}}t_i). \end{aligned} \tag{5.4}$$

Subtracting the last equation for $i = 1$ from those for $i = 2, 3$ eliminates γ and gives a two-by-two linear system for $p_{\mathrm{L}}, q_{\mathrm{L}}$, of determinant

$$-\frac{6(t_1 - t_2)(t_1 - t_3)(t_2 - t_3)\,\mathcal{D}}{d_1 d_2 d_3}, \qquad \mathcal{D} = \sum_i t_i^2 + 4\sum_{i<j} t_i^2 t_j^2 + 12 t_1^2 t_2^2 t_3^2. \tag{5.5}$$

Here $\mathcal{D} > 0$: it is a sum of nonnegative terms which vanishes only if all $t_i = 0$, contrary to their being pairwise distinct. Cramer's rule simplifies to

$$p_{\mathrm{L}} = -\omega\,\frac{2\mathsf{e}_3 - \mathsf{e}_1}{2\mathcal{D}}, \qquad q_{\mathrm{L}} = \omega\,\frac{2\mathsf{e}_2 - 1}{4\mathcal{D}}. \tag{5.6}$$

If $\omega = 0$ then (5.6) gives $X = 0$, hence $x_s = 0$, contradicting regularity of the parameter. Thus $\omega \neq 0$; in particular, the phase ψ is a local parameter rather than an assumption in the calculation.

Step 2: affine compatibility. Differentiating (4.1) and using $t_{i,s} = (1 + t_i^2)\beta_{i,s}$ and the first equation in (5.4) gives

$$\beta_{i,s} = d_i(q_{\mathrm{L}} - p_{\mathrm{L}}t_i) - \omega/2$$

and hence, since $\widehat{n}_i \neq 0$ in the finite chart,

$$\frac{n_{i,s}}{\widehat{n}_i} = \beta_{i,s} - 2t_i\frac{r_{i,s}}{r_i} = d_i\{(1 - 2t_i^2)q_{\mathrm{L}} - 3t_i p_{\mathrm{L}}\} - \omega/2. \tag{5.7}$$

We claim that the right-hand side is an *affine* function of t_i whose coefficients do not depend on i; since $n_i = t_i\widehat{n}_i$, this is precisely the assertion $n_s = \mathfrak{a}n + \mathfrak{b}\widehat{n}$. Indeed, $t_j t_k = \mathsf{e}_2 - t_i(\mathsf{e}_1 - t_i)$, so

$$d_i = 1 + 2\mathsf{e}_2 - 2\mathsf{e}_1 t_i + 2t_i^2.$$

Set $\chi(t) = t^3 - \mathsf{e}_1 t^2 + \mathsf{e}_2 t - \mathsf{e}_3$. Exact polynomial division gives

$$\begin{aligned} &(1 + 2\mathsf{e}_2 - 2\mathsf{e}_1 t + 2t^2)\{(1 - 2t^2)q_{\mathrm{L}} - 3tp_{\mathrm{L}}\} - \frac{\omega}{2}\\ &\quad\equiv \big[-3p_{\mathrm{L}} - 2(\mathsf{e}_1 + 2\mathsf{e}_3)q_{\mathrm{L}}\big]t + (1 + 2\mathsf{e}_2)q_{\mathrm{L}} - 6\mathsf{e}_3 p_{\mathrm{L}} - \frac{\omega}{2} \pmod{\chi(t)}. \end{aligned}$$

Since $\chi(t_i) = 0$, the value in (5.7) is affine in t_i, with

$$\mathfrak{a} = -3p_{\mathrm{L}} - 2(\mathsf{e}_1 + 2\mathsf{e}_3)q_{\mathrm{L}}, \qquad \mathfrak{b} = (1 + 2\mathsf{e}_2)q_{\mathrm{L}} - 6\mathsf{e}_3 p_{\mathrm{L}} - \frac{\omega}{2}. \tag{5.8}$$

Substituting (5.6) into (5.8) and using $\mathcal{D} = \mathsf{e}_1^2 - 2\mathsf{e}_2 + 4\mathsf{e}_2^2 - 8\mathsf{e}_1\mathsf{e}_3 + 12\mathsf{e}_3^2$ yields the exact identity

$$\boxed{\mathfrak{b} = -\omega\,\frac{P_{\mathrm{L}}}{4\mathcal{D}}}, \tag{5.9}$$

where

$$P_{\mathrm{L}} = 1 + 2\sum_i t_i^2 + 2\big[(t_1t_2 + t_1t_3)^2 + (t_1t_2 + t_2t_3)^2 + (t_1t_3 + t_2t_3)^2\big] \geq 1 > 0. \tag{5.10}$$

Together with $\omega \neq 0$ and $\mathcal{D} > 0$, this proves $\mathfrak{b} \neq 0$ throughout the finite chart. Equations (5.5), (5.6), the affine compatibility at the three roots t_i, and (5.9)–(5.10) are independently reconstructed by the sparse-integer certificate `certificates/lami_integer.py` and the exact symbolic rational-function certificate `certificates/lami_symbolic.py`.

Step 3: the projective boundary of the tangent chart. At most one $\cos\beta_i$ can vanish: two vanishing cosines would make the corresponding u_i parallel, putting x on a site line, which is impossible on the fold. Fix a parameter at which $\cos\beta_1 = 0$. Write

$$s_i = \sin\beta_i, \qquad c_i = \cos\beta_i, \qquad \delta_{ij} = s_ic_j - s_jc_i, \qquad \varepsilon_* = s_1 \in \{\pm 1\}.$$

Thus $c_2c_3 \neq 0$, and t_2, t_3 remain valid coordinates. Define

$$\overline{d}_1 = c_2c_3 + 2s_2s_3$$

and

$$\begin{aligned}\overline{\mathcal{D}} = {}& s_1^2c_2^2c_3^2 + s_2^2c_1^2c_3^2 + s_3^2c_1^2c_2^2 \\ &+ 4\big(s_1^2s_2^2c_3^2 + s_1^2s_3^2c_2^2 + s_2^2s_3^2c_1^2\big) + 12s_1^2s_2^2s_3^2.\end{aligned}$$

We first treat this boundary directly, without assuming that its zero set is isolated. One denominator-cleared determinant of the two equations used in Step 1 is

$$6(t_1 - t_2)(t_2 - t_3)(t_3 - t_1)d_1\mathcal{D}.$$

After substituting $t_i = s_i/c_i$ and multiplying by $c_1^4c_2^5c_3^5$, its exact homogeneous form is

$$\overline{J} = 6\delta_{12}\delta_{23}\delta_{31}\,\overline{d}_1\overline{\mathcal{D}}. \tag{5.11}$$

At $c_1 = 0$, the homogeneous form of (5.2) gives

$$\overline{d}_1 = 3\lambda_1c_2c_3, \qquad 1 + 2t_2t_3 = 3\lambda_1 \neq 0.$$

Moreover,

$$\delta_{23} = c_2c_3(t_2 - t_3) \neq 0, \qquad \overline{\mathcal{D}} = c_2^2c_3^2D_\infty, \qquad D_\infty = 1 + 4t_2^2 + 4t_3^2 + 12t_2^2t_3^2 > 0.$$

Here $t_2 \neq t_3$ because equality would put x on the site line through a_2, a_3. Since $\delta_{12} = \varepsilon_*c_2$ and $\delta_{31} = -\varepsilon_*c_3$, equation (5.11) yields

$$\overline{J}\Big| * c_1 = 0 = -18\lambda_1(t_2 - t_3)c_2^5c_3^5D * \infty \neq 0.$$

We now display explicitly the regularized system whose determinant is being used. Work in the local chart $s_1c_2c_3 \neq 0$ and put

$$\tau = \frac{c_1}{s_1} = \frac{1}{t_1}, \qquad u = t_2, \qquad v = t_3,$$

together with

$$D_\tau = D_\infty + \tau^2(u^2 + v^2 + 4u^2v^2) = \frac{\mathcal{D}}{t_1^2}.$$

Regularize the common radial factor and the velocity by defining

$$\widetilde{C} = \frac{r_1 \overline{d}_1}{s_1 c_2 c_3} = \frac{r_1(1+2uv)}{s_1}, \qquad \frac{X}{\widetilde{C}} = \widetilde{p} + i\widetilde{q}.$$

These quantities are well defined in a neighbourhood of the boundary point. When $\tau \neq 0$, they agree with $\widetilde{C} = C/t_1$, $\widetilde{p} = t_1 p_{\mathrm{L}}$, and $\widetilde{q} = t_1 q_{\mathrm{L}}$. Write the identities used in Step 1 in the homogeneous direction coordinates (s_i, c_i), differentiate them, substitute $z_{i,s} = X - i\omega z_i/2$, and eliminate the logarithmic derivative of the common radial factor. Subtracting the equation with $i = 1$ from those with $i = 2, 3$ gives the polynomial system

$$M(\tau, u, v)\begin{pmatrix}\widetilde{p}\\ \widetilde{q}\end{pmatrix} = -\frac{\omega}{2}\begin{pmatrix}2v^2-1\\ 2u^2-1\end{pmatrix}, \tag{5.12}$$

where

$$M(\tau, u, v) = \begin{pmatrix} m_{21} & m_{22}\\ m_{31} & m_{32}\end{pmatrix}$$

and

$$\begin{aligned} m_{21} &= 1 + 4v^2 + 12uv^3 + \tau(u + 4uv^2 - 2v - 2v^3),\\ m_{22} &= 4uv^2 + 4u - 8v^3 - 2v - \tau(8uv^3 + 2uv + 6v^2),\\ m_{31} &= 1 + 4u^2 + 12u^3v + \tau(-2u^3 + 4u^2v - 2u + v),\\ m_{32} &= -8u^3 + 4u^2v - 2u + 4v - \tau(8u^3v + 6u^2 + 2uv). \end{aligned}$$

For comparison with the finite-chart calculation, if E_i denotes the left-hand side obtained by moving every term of the third equation in (5.4) to one side after substituting its first equation, then, for $\tau \neq 0$,

$$E_2 - E_1 = \frac{\tau u - 1}{(\tau + 2v)(1+2uv)} G_2, \qquad E_3 - E_1 = \frac{\tau v - 1}{(\tau + 2u)(1+2uv)} G_3,$$

where $(G_2, G_3)^\mathsf{T}$ is the left-hand side of (5.12). Before division, the homogeneous denominator-cleared identities are

$$(\tau u - 1)G_2 = 0, \qquad (\tau v - 1)G_3 = 0.$$

The two prefactors equal -1 at $\tau = 0$ and are therefore units near the boundary point. Thus (5.12) remains valid there without any assumption that the zero of c_1 is isolated. Its determinant is the exact polynomial

$$\det M(\tau, u, v) = -6(u - v)(1 + 2uv)D_\tau. \tag{5.13}$$

The connection with the homogeneous determinant (5.11) is

$$\overline{J} = s_1^4 c_2^5 c_3^5 (1-\tau u)(1-\tau v) \det M(\tau,u,v).$$

At $\tau = 0$, therefore,

$$\det M(0,u,v) = -6(u-v)(1+2uv)D_\infty = -18\lambda_1(u-v)D_\infty \neq 0.$$

Thus the boundary system has a unique Cramer solution, with no transversality assumption. Exact simplification gives

$$\widetilde{p} = -\omega\frac{(2uv-1)-\tau(u+v)}{2D_\tau}, \qquad \widetilde{q} = \omega\frac{2(u+v)+\tau(2uv-1)}{4D_\tau}.$$

At $\tau = 0$, where $s_1 = \varepsilon_*$, the boundary values are

$$\widetilde{C} = \varepsilon_* r_1(1+2uv), \qquad \widetilde{p} = -\omega\frac{2uv-1}{2D_\infty}, \qquad \widetilde{q} = \omega\frac{u+v}{2D_\infty}.$$

Restoring $u = t_2$ and $v = t_3$, the identity $X = C(p_{\mathrm{L}} + iq_{\mathrm{L}}) = \widetilde{C}(\widetilde{p} + i\widetilde{q})$ specializes to

$$X = \omega\Lambda_*, \qquad \Lambda_* = \frac{\varepsilon_* r_1(1+2t_2t_3)}{2D_\infty}\left[-(2t_2t_3-1) + i(t_2+t_3)\right] \neq 0. \tag{5.14}$$

Indeed, the squared modulus of the bracket is $1 + (t_2 - t_3)^2 + 4t_2^2t_3^2 > 0$, while all the other factors in Λ_* have already been shown nonzero. Regularity gives $X \neq 0$, so (5.14) forces $\omega \neq 0$. Since $z_1 = i\varepsilon_* r_1$, the identity $z_{1,s} = X - i\omega z_1/2$ and (5.14) give

$$\beta_{1,s} = \Im(X/z_1) - \omega/2 = -\omega\frac{(1+2t_2^2)(1+2t_3^2)}{D_\infty} \neq 0.$$

Consequently

$$(\cos\beta_1)*s = -\sin\beta_1\,\beta*1, s = -\varepsilon_*\beta_{1,s} \neq 0,$$

so this zero is simple. The other two boundary charts are identical after cyclic relabelling. Thus the set on a fold circle where some $\cos\beta_i$ vanishes is closed and discrete. Because the fold circle is compact, this set is finite.

In a punctured neighborhood of each such parameter the finite-chart formula (5.9) applies, and exact division of its two polynomials gives

$$\frac{P_{\mathrm{L}}}{4\mathcal{D}} \longrightarrow \frac{2+4(t_2^2+t_2t_3+t_3^2)}{4D_\infty} > 0. \tag{5.15}$$

The coefficients $\mathfrak{a}, \mathfrak{b}$ are smooth by the formulas at the beginning of the proof. Therefore continuity, (5.9), and (5.15) give at the boundary point

$$\mathfrak{b} = -\omega\,\frac{2+4(t_2^2+t_2t_3+t_3^2)}{4D_\infty} \neq 0.$$

The regularized system (5.12), its determinant and Cramer solution, the exact X/ω transition, and the $P_{\mathrm{L}}/\mathcal{D}$ limit are reconstructed in `certificates/lami_symbolic.py`; the independently cleared homogeneous determinant and its projective boundary specialization are verified in `certificates/lami_projective.py`.

We have therefore proved globally that $n_s = \mathfrak{a}n + \mathfrak{b}\widehat{n}$ with $\mathfrak{b} \neq 0$, and then $n \times n_s = \mathfrak{b}\, n \times \widehat{n} \neq 0$ by Lemma 4.1. $\square$

5.1 The affine charge chart

Fix the chamber signs $\sigma_i = \operatorname{sign}\lambda_i$, set $D_\sigma = \operatorname{diag}(\sigma_1, \sigma_2, \sigma_3)$, $\mathbf{1} = (1,1,1)$, and $\mathsf{z}_0 = \mathbf{1}/3$. Consider the projective chart

$$U_\sigma = \{[q] \in \mathbb{RP}^2 : \langle \sigma, q \rangle \neq 0\}.$$

The representative-independent formula

$$\mathsf{z}([q]) = \frac{D_\sigma q}{\langle \sigma, q \rangle}$$

defines a real-analytic bijection

$$U_\sigma \longrightarrow H := \{\mathsf{z} \in \mathbb{R}^3 : \mathbf{1} \cdot \mathsf{z} = 1\},$$

whose inverse is $\mathsf{z} \mapsto [D_\sigma \mathsf{z}]$. Let $\mathsf{E} \colon \mathbb{R}^2 \to \mathbf{1}^\perp$ be the isomorphism $\mathsf{E}(y_1, y_2) = (y_1, y_2, -y_1 - y_2)$. Every $\mathsf{z} \in H$ has the unique expression

$$\mathsf{z} = \mathsf{z}_0 + \mathsf{E}y, \qquad y = (\mathsf{z}_1 - 1/3, \mathsf{z}_2 - 1/3).$$

For every x in the fixed strict sign chamber put $\nu(x) = \vartheta(x)$ and

$$M_\sigma(x) = \langle \sigma, \nu(x) \rangle = \sum_i |\lambda_i(x)| r_i(x)^3 > 0.$$

Thus $\Theta(x) \in U_\sigma$ and

$$\mathsf{z}(\Theta(x)) * i = \frac{|\lambda_i(x)| r_i(x)^3}{M * \sigma(x)} > 0.$$

There is consequently a unique real-analytic map Θ_σ on the whole chamber such that $\mathsf{z}(\Theta(x)) = \mathsf{z}_0 + \mathsf{E}\Theta_\sigma(x)$; its image lies in the interior of the standard affine simplex in H.

On the fold put $\widetilde{n} = D_\sigma n$. Since $q = \langle \sigma, q \rangle D_\sigma \mathsf{z}$, the projective line

$$L_s = \{[q] \in \mathbb{RP}^2 : \langle n, q \rangle = 0\}$$

has affine equation

$$\mathbf{N} \cdot y + c_{\mathrm{aff}} = 0, \qquad \mathbf{N} = \mathsf{E}^{\mathsf{T}} \widetilde{n} = (\widetilde{n}_1 - \widetilde{n}_3, \widetilde{n}_2 - \widetilde{n}_3), \qquad c_{\mathrm{aff}} = \frac{\widetilde{n}_1 + \widetilde{n}_2 + \widetilde{n}_3}{3}.$$

Changing a local phase lift by $\psi \mapsto \psi + 2\pi$ sends $(\widetilde{n}, \mathbf{N}, c_{\mathrm{aff}})$ to its simultaneous negative. It therefore leaves both this affine line and $\det(\mathbf{N}, \mathbf{N}_s)$ unchanged.

Lemma 5.2 (Regularity of the dual line)**.** *For all $a, b \in \mathbb{R}^3$ one has $\det(\mathsf{E}^{\mathsf{T}} a, \mathsf{E}^{\mathsf{T}} b) = \mathbf{1} \cdot (a \times b)$; consequently, for every regular local parameter s on a fold circle,*

$$\det(\mathbf{N}, \mathbf{N}_s) = (\sigma_1\sigma_2\sigma_3)\langle n \times n_s, \sigma \rangle = -(\sigma_1\sigma_2\sigma_3)\frac{2S\,\mathfrak{b}}{(r_1 r_2 r_3)^3} M_\sigma \neq 0. \tag{5.16}$$

Proof. The first identity is a direct expansion of both sides. For every invertible matrix A, the general transformation law is

$$(Aa) \times (Ab) = \det(A) A^{-\mathsf{T}} (a \times b).$$

Applying the first identity to $\widetilde{n} = D_\sigma n$, $\widetilde{n}_s = D_\sigma n_s$, and then using $D_\sigma^{-\mathsf{T}} = D_\sigma$ and $\mathbf{1}^\mathsf{T} D_\sigma = \sigma^\mathsf{T}$ gives the middle expression in (5.16). The last equality follows from $n \times n_s = \mathfrak{b}\, n \times \widehat{n}$, Lemma 4.1 and $\langle \sigma, \nu \rangle = M_\sigma$; it is nonzero by Proposition 5.1. □

6 Absolute degree one and the support graph

Proposition 6.1 (Support function)**.** *Fix a disc Ω in the strict sign chamber with sign vector σ, and let $x(t)$, $t \in \mathbb{R}$, be a positively oriented once-around regular parametrization of $\partial\Omega$ with period T_0; that is, $x \colon \mathbb{R}/T_0\mathbb{Z} \to \partial\Omega$ is an orientation-preserving smooth diffeomorphism. Orient $\mathbb{RP}^1$ by increasing angle modulo π. Then*

$$[\mathbf{N}] \colon \partial\Omega \longrightarrow \mathbb{RP}^1$$

is a real-analytic diffeomorphism of degree

$$\varepsilon_\mathbf{N} := \deg([\mathbf{N}]) = -\sigma_1\sigma_2\sigma_3.$$

On the universal cover, choose any phase lift ψ satisfying $3\Xi(x(t)) = e^{i\psi(t)}$, form $(\mathbf{N}, c_{\mathrm{aff}})$ from that lift as above, and choose any real angle θ satisfying $\mathbf{N}/|\mathbf{N}| = \mathbf{u}(\theta)$. Then θ is a regular parameter and satisfies $\theta(t + T_0) = \theta(t) + \varepsilon_\mathbf{N}\pi$. The formula

$$h(\theta(t)) = -c_{\mathrm{aff}}(t)/|\mathbf{N}(t)|$$

defines a choice-independent real-analytic function on $\mathbb{R}/2\pi\mathbb{Z}$ with $h(\theta + \pi) = -h(\theta)$, and the affine caustic $\Gamma(t) = \Theta_\sigma(x(t))$ satisfies

$$\Gamma(\theta) = h(\theta)\mathbf{u}(\theta) + h'(\theta)\mathbf{v}(\theta), \qquad \Gamma'(\theta) = \rho(\theta)\mathbf{v}(\theta), \qquad \rho = h + h'', \tag{6.1}$$

where $\mathbf{u}(\theta) = (\cos\theta, \sin\theta)$ and $\mathbf{v}(\theta) = (-\sin\theta, \cos\theta)$, and primes denote θ-derivatives. Moreover, $\Gamma(\theta + \pi) = \Gamma(\theta)$ and $\rho(\theta + \pi) = -\rho(\theta)$.

Proof. For arbitrary x in the strict sign chamber and arbitrary $\phi \in \mathbb{R}$, define

$$n_i(x, \phi) = \frac{\Im(e^{-i\phi}(x - a_i))}{r_i^3}, \qquad \widetilde{n} = D_\sigma n, \qquad \mathbf{N} = \mathsf{E}^\mathsf{T}\widetilde{n}.$$

If $\mathbf{N} = 0$, then $\widetilde{n} \in \ker(\mathsf{E}^\mathsf{T}) = \mathbb{R}\mathbf{1}$, so $n = g_0\sigma$. Barycentric closure gives

$$0 = \Im\left(e^{-i\phi}\sum_i \lambda_i(x - a_i)\right) = \langle \nu, n \rangle = g_0 M_\sigma,$$

hence $g_0 = 0$. But $n = 0$ would make all three vectors $e^{-i\phi}(x - a_i)$ real and force the sites to be collinear. Thus $\mathbf{N}(x, \phi) \neq 0$ throughout the chamber.

Along the fold choose ψ by $3\Xi(x(t)) = e^{i\psi(t)}$. Because $x(t)$ traverses the positively oriented fold circle once, (3.12) gives $\psi(t + T_0) = \psi(t) - 2\pi$. The sign chamber is convex, its defining barycentric inequalities being affine, so for a fixed x_* in it the straight contraction $x_\tau(t) = (1 - \tau)x(t) + \tau x_*$ stays in the chamber. Putting $\phi(t) = \psi(t)/2$ gives a nonvanishing homotopy $[\mathbf{N}(x_\tau(t), \phi(t))]$ of projective loops. Here ϕ is merely an auxiliary angle away from the fold.

At x_* put $u_{i,*} = x_* - a_i$, $r_{i,*} = |u_{i,*}|$, and

$$n_i^0 = \frac{\Im u_{i,*}}{r_{i,*}^3}, \qquad \widehat{n}_i^0 = \frac{\Re u_{i,*}}{r_{i,*}^3}, \qquad \mathbf{C}_0 = \mathsf{E}^\mathsf{T} D_\sigma n^0, \qquad \mathbf{S}_0 = -\mathsf{E}^\mathsf{T} D_\sigma \widehat{n}^0.$$

Then

$$\mathbf{N}(x_*, \phi) = \mathbf{C}_0 \cos\phi + \mathbf{S}_0 \sin\phi.$$

For cyclic (i, j, k), barycentric geometry gives

$$(n^0 \times (-\widehat{n}^0)) * i = \frac{\det(u * j, *, u_{k,*})}{r_{j,*}^3 r_{k,*}^3} = \frac{2S\lambda_i(x_*)}{r_{j,*}^3 r_{k,*}^3}.$$

Consequently,

$$n^0 \times (-\widehat{n}^0) = \frac{2S}{(r_{1,*} r_{2,*} r_{3,*})^3}\, \nu(x_*).$$

Using the first identity of Lemma 5.2 and the cross-product transformation law from its proof now gives

$$\begin{aligned}\det(\mathbf{C}_0, \mathbf{S}_0) &= \mathbf{1} \cdot ((D_\sigma n^0) \times (-D_\sigma \widehat{n}^0)) \\ &= (\sigma_1\sigma_2\sigma_3) \left\langle \sigma, n^0 \times (-\widehat{n}^0) \right\rangle \\ &= (\sigma_1\sigma_2\sigma_3) \frac{2S\, M_\sigma(x_*)}{(r_{1,*} r_{2,*} r_{3,*})^3} \neq 0.\end{aligned}$$

Thus the endpoint loop is the composition of $[\cos\phi : \sin\phi]$ with the projective automorphism having columns $\mathbf{C}_0, \mathbf{S}_0$. The latter has degree sign $\det(\mathbf{C}_0, \mathbf{S}_0) = \sigma_1\sigma_2\sigma_3$, whereas $\phi(t+T_0) = \phi(t) - \pi$. Homotopy invariance therefore gives

$$\deg([\mathbf{N}]) = -\sigma_1\sigma_2\sigma_3.$$

By (5.16), $\theta_t = \det(\mathbf{N}, \mathbf{N}_t)/|\mathbf{N}|^2 \neq 0$ for a local normal-angle lift, so $[\mathbf{N}]$ is a local diffeomorphism of circles; its image is open and, by compactness, closed. Since $\mathbb{RP}^1$ is connected, the map is onto. It is therefore a finite covering, and $|\deg([\mathbf{N}])| = 1$ makes it one-sheeted, hence a global diffeomorphism.

This diffeomorphism is intrinsically real analytic. Indeed, $\partial\Omega$ is a real-analytic one-manifold because it is a regular level of the real-analytic function $|\Xi|^2$. In a local real-analytic parameter s, choose a real-analytic phase lift. Then $\mathbf{N}, c_{\text{aff}}$, and a local normal angle θ are real analytic, and

$$\theta_s = \frac{\det(\mathbf{N}, \mathbf{N}_s)}{|\mathbf{N}|^2} \neq 0.$$

The real-analytic inverse function theorem therefore gives a real-analytic inverse normal-angle coordinate.

All vector lifts are now taken on the universal cover. The half-angle formula gives $(\mathbf{N}, c_{\text{aff}})(t + T_0) = -(\mathbf{N}, c_{\text{aff}})(t)$. Put $\mathbf{U} = \mathbf{N}/|\mathbf{N}|$ and choose $\theta : \mathbb{R} \to \mathbb{R}$ with $\mathbf{U}(t) = \mathbf{u}(\theta(t))$. Then $\theta(t + T_0) = \theta(t) + \varepsilon_{\mathbf{N}}\pi$ and $\theta_t \neq 0$. Thus θ is strictly monotone, while its quasi-periodicity makes its image unbounded in both directions; consequently $\theta\colon \mathbb{R} \to \mathbb{R}$ is a diffeomorphism. Define h by the displayed formula in the statement. The anti-periodicity of $(\mathbf{N}, c_{\text{aff}})$ gives

$$h(\theta + \pi) = -h(\theta), \qquad h(\theta + 2\pi) = h(\theta),$$

and the preceding analytic inverse-function argument shows that h is real analytic in θ, independently of the auxiliary smooth parameter t. Changing the phase lift by 2π replaces $(\mathbf{N}, c_{\text{aff}}, \mathbf{U}, \theta)$ by $(-\mathbf{N}, -c_{\text{aff}}, -\mathbf{U}, \theta + \pi)$, while changing the angle lift adds a multiple of 2π. The two displayed transformation laws therefore show that h is choice-independent on the oriented normal double cover $\mathbb{R}/2\pi\mathbb{Z}$.

By Lemma 4.1 and the definition of Θ_σ,

$$\mathsf{z}_0 + \mathsf{E}\Gamma = \frac{D_\sigma \nu}{M_\sigma},$$

and hence

$$\mathbf{N}\cdot\Gamma + c_{\mathrm{aff}} = \frac{\langle n, \nu\rangle}{M_\sigma} = 0, \qquad \mathbf{N}_t\cdot\Gamma + (c_{\mathrm{aff}}) * t = \frac{\langle n_t, \nu\rangle}{M * \sigma} = 0.$$

In the second equation the caustic point is held fixed while only the line coefficients are differentiated. Because $\det(\mathbf{N}, \mathbf{N}_t) \neq 0$, these two equations uniquely identify the actual caustic point with the envelope of the line family, including at cusp parameters. Differentiating the first line equation along the actual caustic and comparing with the second gives $\mathbf{N}\cdot\Gamma_t = 0$. After unit normalization and reparametrization by θ this gives

$$\mathbf{u}\cdot\Gamma = h, \qquad \mathbf{u}\cdot\Gamma' = 0.$$

Differentiating the first identity with respect to θ gives $\mathbf{v}\cdot\Gamma = h'$. Resolving Γ in the orthonormal basis $(\mathbf{u}, \mathbf{v})$ proves the first identity in (6.1):

$$\Gamma = h\mathbf{u} + h'\mathbf{v}.$$

Differentiating it proves the second:

$$\Gamma' = h'\mathbf{u} + h\mathbf{v} + h''\mathbf{v} - h'\mathbf{u} = (h + h'')\mathbf{v}.$$

Under $\theta \mapsto \theta + \pi$, each factor in both products of the first formula changes sign. Hence Γ is π-periodic; since h and h'' are both π-antiperiodic, so is $\rho = h + h''$. $\square$

7 Exactly three cusps

Work in the affine charge chart of Subsection 5.1. For a fixed strict sign chamber, write

$$q(y) = D_\sigma(\mathsf{z}_0 + \mathsf{E}y), \qquad y \in \mathbb{R}^2,$$

and set $\mathcal{A}(x) = D_y \nabla_P V_{q(y)}(x)$. The matrix $\mathcal{A}$ is independent of y because V_q is linear in q. From the definition of the charge-variation map in Lemma 2.3,

$$\mathcal{A}(x)v = K_x(D_\sigma \mathsf{E}v).$$

It is therefore invertible throughout the strict chamber: if $\mathcal{A}(x)v = 0$ then the charge variation $D_\sigma\mathsf{E}v$ lies in $\ker K_x = \mathbb{R}\nu$, while $\langle\sigma, D_\sigma\mathsf{E}v\rangle = \mathbf{1}\cdot\mathsf{E}v = 0$ and $\langle\sigma,\nu\rangle = M_\sigma(x) > 0$; hence $D_\sigma\mathsf{E}v = 0$ and $v = 0$. Linearity in the charges and vanishing at $y = \Theta_\sigma(x)$ give the exact incidence identity

$$\nabla_P V_{q(y)}(x) = \mathcal{A}(x)\{y - \Theta_\sigma(x)\}. \tag{7.1}$$

Let $H(x)$ denote the planar Hessian of $V_{q(\Theta_\sigma(x))}$ at x with the charge *held fixed* while the spatial second derivative is taken. Since $q(\Theta_\sigma(x)) = \nu(x)/M_\sigma(x)$, Lemma 2.3 gives $H = H_0/M_\sigma$ and therefore

$$\det H = \frac{1 - 9|\Xi|^2}{4M_\sigma^2}.$$

In particular, H is positive definite on Ω. Differentiating (7.1) on the incidence graph gives

$$H + \mathcal{A}\, d\Theta_\sigma = 0, \tag{7.2}$$

so $\ker d\Theta_{\sigma,x} = \ker H(x)$ and $\det d\Theta_\sigma = \det H / \det \mathcal{A}$. By Proposition 3.5 the differential $d|\Xi|^2$ does not vanish on $\partial\Omega$; since $M_\sigma > 0$ and $\det \mathcal{A} \neq 0$, the Jacobian determinant of Θ_σ vanishes simply there. Proposition 3.5 also shows that $\partial\Omega$ is exactly the singular curve of Θ_σ in the chamber.

7.1 Classification of the boundary singularities

Fix $x_0 \in \partial\Omega$, put $y_0 = \Theta_\sigma(x_0)$, and let $V = V_{q(y_0)}|_P$ with x_0 translated to the origin; all directional derivatives below are of this fixed-charge function. Choose an orthonormal basis (e, f) with e spanning the null line of $H(x_0)$. The eigenvalues of H_0 on the fold are 0 and 1, so

$$\kappa := V_{ff} = \frac{1}{M_\sigma(x_0)} > 0.$$

Thus $V_e = V_f = V_{ee} = V_{ef} = 0$ at the origin.

Lemma 7.1 (Fold criterion)**.** *$e(\det H) = \kappa V_{eee}$ at x_0. Hence the null line is transverse to $\partial\Omega$ exactly when $V_{eee} \neq 0$, and tangent exactly when $V_{eee} = 0$.*

Proof. At x_0 one has $H = \operatorname{diag}(0, \kappa)$ in the basis (e, f), so $\operatorname{adj} H = \operatorname{diag}(\kappa, 0)$ and $e(\det H) = \operatorname{tr}\big(\operatorname{adj} H \cdot e(H)\big) = \kappa\, e(H_{ee})$. Now $H_{ee}(x) = \partial_e^2 V_{q(\Theta_\sigma(x))}(x)$ depends on x both through the evaluation point and through the charge; the second contribution is $\partial_e^2 V_{\dot q}$ with $\dot q = D_\sigma \mathsf{E}\, d\Theta_{\sigma,x_0}(e) = 0$, because $e \in \ker d\Theta_{\sigma,x_0}$ by (7.2). Hence $e(H_{ee}) = V_{eee}$. Finally, $\partial\Omega = \{\det H = 0\}$ near x_0 and $\det H$ vanishes simply there. $\square$

Call a boundary point with $V_{eee} = 0$ a *candidate cusp*. Give the null coordinate ξ weight one and the transverse coordinate η weight two. At an arbitrary boundary point, the Taylor expansion has the form

$$V(\xi e + \eta f) = V(0) + \frac{\kappa}{2}\eta^2 + \frac{V_{eee}}{6}\xi^3 + \frac{V_{eef}}{2}\xi^2\eta + \frac{V_{eeee}}{24}\xi^4 + O_{\mathrm{wt}}(5).$$

Here $O_{\mathrm{wt}}(5)$ denotes terms of weighted degree at least five. At a candidate cusp $V_{eee} = 0$. Since $\kappa \neq 0$, the real-analytic implicit function theorem gives a unique local solution of $V_f = 0$ of the form $\eta(\xi) = -V_{eef}\xi^2/(2\kappa) + O(\xi^3)$. Substituting it into V gives

$$V(\xi e + \eta(\xi) f) = V(0) + \frac{V_{eee}}{6}\xi^3 + c_4\xi^4 + O(\xi^5), \qquad c_4 = \frac{1}{24}\left(V_{eeee} - \frac{3V_{eef}^2}{\kappa}\right).$$

Write the vectors from the equilibrium to the sites as $r_i(c_i, s_i)$ with $c_i = \cos\theta_i$ and $s_i = \sin\theta_i$. The sourcewise Coulomb derivatives, obtained from the multipole expansion $|x - a_i|^{-1} = \sum_{n\geq 0} |x|^n r_i^{-n-1} P_n(\cos\gamma_i)$ about x_0, in which γ_i is the angle at x_0 between $x - x_0$ and $a_i - x_0$, are

$$
\begin{aligned}
V_e &= \sum_i \frac{q_i}{r_i^2} c_i, & V_f &= \sum_i \frac{q_i}{r_i^2} s_i,\\
V_{ee} &= 2\sum_i \frac{q_i}{r_i^3} P_2(c_i), & V_{ef} &= 3\sum_i \frac{q_i}{r_i^3} c_i s_i,\\
V_{eee} &= 6\sum_i \frac{q_i}{r_i^4} P_3(c_i), & V_{eef} &= 3\sum_i \frac{q_i}{r_i^4} s_i(5c_i^2-1),\\
V_{eeee} &= 24\sum_i \frac{q_i}{r_i^5} P_4(c_i),
\end{aligned}
$$

where P_j is the jth Legendre polynomial. These formulas are checked term by term in `certificates/coulomb_derivatives.py`.

For cyclic (i,j,k) put

$$
\mathfrak{d}_i = \sin(\theta_k-\theta_j), \qquad \mathfrak{D} = \mathfrak{d}_1\mathfrak{d}_2\mathfrak{d}_3, \qquad \mathfrak{p}_i = 2c_jc_k + s_js_k.
$$

The three unit direction vectors (c_i,s_i) span $\mathbb{R}^2$; otherwise the three sites would lie on a single line through x_0. Hence the two-by-three equilibrium matrix has rank two, and its kernel is generated by $(\mathfrak{d}_1,\mathfrak{d}_2,\mathfrak{d}_3)$. The equilibrium equations therefore give $q_i/r_i^2 = \gamma_*\mathfrak{d}_i$ for a unique $\gamma_*\neq 0$. Since every $q_i\neq 0$, all $\mathfrak{d}_i\neq 0$, so the three directions $e^{2i\theta_i}$ are distinct. The two null-Hessian equations $V_{ee}=V_{ef}=0$ read

$$
\sum_i \frac{\mathfrak{d}_i P_2(c_i)}{r_i} = 0, \qquad \sum_i \frac{\mathfrak{d}_i c_i s_i}{r_i} = 0.
$$

Their two-by-three coefficient matrix has rank two. Otherwise some $(\alpha,\beta)\neq(0,0)$ would satisfy $\alpha P_2(c_i)+\beta c_i s_i = 0$ for all i; in the coordinates $(X_i,Y_i) = (\cos 2\theta_i, \sin 2\theta_i)$, and using $P_2(c) = (1+3X)/4$ and $cs = Y/2$, this is the nonzero affine line $\alpha(1+3X)+2\beta Y = 0$ through three distinct points of the unit circle, which is impossible. Direct substitution gives the exact identities

$$
\sum_i \mathfrak{d}_i P_2(c_i)\mathfrak{p}_i = 0, \qquad \sum_i \mathfrak{d}_i c_i s_i \mathfrak{p}_i = 0, \qquad \sum_i \mathfrak{d}_i\mathfrak{p}_i = -3\mathfrak{D}.
$$

The third identity shows that $(\mathfrak{d}_i\mathfrak{p}_i)_i$ is nonzero, and the first two show that it lies in the common kernel. Since that kernel is one-dimensional, there is a $\tau_0\neq 0$ such that $\mathfrak{d}_i/r_i = \tau_0\mathfrak{d}_i\mathfrak{p}_i$ for every i. Since every $\mathfrak{d}_i\neq 0$, it follows that

$$
\frac{1}{r_i} = \tau_0\,\mathfrak{p}_i, \qquad \tau_0\neq 0,
$$

and in particular every $\mathfrak{p}_i\neq 0$. Define

$$
\begin{aligned}
\widehat{E} &= \sum_i \mathfrak{d}_i\mathfrak{p}_i^2 P_3(c_i), & \widehat{U} &= \sum_i \mathfrak{d}_i\mathfrak{p}_i^2 s_i(5c_i^2-1),\\
\widehat{W} &= \sum_i \mathfrak{d}_i\mathfrak{p}_i^3 P_4(c_i), & \mathcal{I} &= 3\widehat{U}^2 + 8\mathfrak{D}\widehat{W}.
\end{aligned}
$$

Using $\sum_i \mathfrak{d}_i\mathfrak{p}_i = -3\mathfrak{D}$ and harmonicity (which gives $\kappa = V_{ff} = \sum_i q_i/r_i^3$ when $V_{ee}=0$), the derivative formulas give

$$
\begin{aligned}
\kappa &= -3\gamma_*\tau_0\mathfrak{D}, & V_{eee} &= 6\gamma_*\tau_0^2\widehat{E},\\
V_{eef} &= 3\gamma_*\tau_0^2\widehat{U}, & V_{eeee} &= 24\gamma_*\tau_0^3\widehat{W}.
\end{aligned}
$$

With $\varpi = \gamma_* \tau_0^2 \neq 0$, substitution yields

$$\kappa c_4 = -\frac{3}{8}\varpi^2 \mathcal{I}. \tag{7.3}$$

Lemma 7.2 (Strict positivity)**.** *At every candidate cusp, $\kappa c_4 < 0$.*

Proof. Set

$$\begin{aligned}
\Upsilon_0 &= c_1c_2c_3, \qquad \Upsilon_3 = s_1s_2s_3,\\
\Upsilon_1 &= s_1c_2c_3 + c_1s_2c_3 + c_1c_2s_3,\\
\mathcal{C} &= s_1s_2c_3 + s_1c_2s_3 + c_1s_2s_3 - 2\Upsilon_0,\\
\mathcal{F} &= 12\Upsilon_1^2 - 14\Upsilon_1\Upsilon_3 + 3\Upsilon_3^2 + 8\Upsilon_0^2.
\end{aligned}$$

Exact Laurent-polynomial expansion gives

$$\widehat{E} = -\mathfrak{D}\,\mathcal{C}, \qquad \widehat{U} = 4\mathfrak{D}\,\Upsilon_1, \qquad \mathcal{I} = \mathfrak{D}^2\{2\mathcal{F} - 8\mathcal{C}(\mathcal{C} + 7\Upsilon_0)\}.$$

The candidate-cusp condition is $\widehat{E} = 0$; since $\mathfrak{D} \neq 0$ this means $\mathcal{C} = 0$, and then $\mathcal{I} = 2\mathfrak{D}^2\mathcal{F}$.

If $\Upsilon_0 \neq 0$, put $t_i = \tan\theta_i$ and let $\mathsf{e}_1, \mathsf{e}_2, \mathsf{e}_3$ be their elementary symmetric functions. Then $\mathcal{C} = 0$ reads $\mathsf{e}_2 = 2$, and

$$\begin{aligned}
\frac{\mathcal{F}}{\Upsilon_0^2} &= 12\mathsf{e}_1^2 - 14\mathsf{e}_1\mathsf{e}_3 + 3\mathsf{e}_3^2 + 8\\
&= \frac{184}{3} + 12(\mathsf{e}_1^2 - 3\mathsf{e}_2) + \frac{14}{3}(\mathsf{e}_2^2 - 3\mathsf{e}_1\mathsf{e}_3) + 3\mathsf{e}_3^2 > 0,
\end{aligned}$$

because

$$\begin{aligned}
\mathsf{e}_1^2 - 3\mathsf{e}_2 &= \tfrac{1}{2}\textstyle\sum_{i<j}(t_i - t_j)^2,\\
\mathsf{e}_2^2 - 3\mathsf{e}_1\mathsf{e}_3 &= \tfrac{1}{2}\big[(t_1t_2 - t_1t_3)^2 + (t_1t_2 - t_2t_3)^2 + (t_1t_3 - t_2t_3)^2\big].
\end{aligned}$$

If $\Upsilon_0 = 0$, at most one cosine vanishes because the directions $e^{2i\theta_i}$ are distinct. By symmetry, take $c_3 = 0$, so $s_3 = \pm 1$ and $\mathcal{C} = s_3\sin(\theta_1 + \theta_2)$. Thus $\mathcal{C} = 0$ forces $\theta_2 \equiv -\theta_1 \pmod{\pi}$. Consequently, for some $\varepsilon \in \{\pm 1\}$, $c_2 = \varepsilon c_1$ and $s_2 = -\varepsilon s_1$, and hence

$$\mathcal{F} = 12c_1^2c_2^2 - 14c_1c_2s_1s_2 + 3s_1^2s_2^2 = 12c_1^4 + 14c_1^2s_1^2 + 3s_1^4 = c_1^4 + 8c_1^2 + 3 > 0.$$

In both cases $\mathcal{I} = 2\mathfrak{D}^2\mathcal{F} > 0$, so (7.3) gives $\kappa c_4 < 0$.

The angular-kernel identities, the homogeneous factorization of $\mathcal{I}$, the normalization (7.3), and both strict-positivity charts are independently reconstructed by `certificates/cusp_quartic.py`. □

Proposition 7.3 (Boundary singularities)**.** *Every singularity of Θ_σ on $\partial\Omega$ is either a fold ($V_{eee} \neq 0$) or an ordinary Whitney cusp ($V_{eee} = 0$). In Arnold's notation [2], the reduced potential at a cusp has type A_3; types A_k with $k \geq 4$ do not occur.*

Proof. On the fold, $d\Theta_\sigma$ has rank one and its Jacobian vanishes simply, so its singular locus is a smooth curve. The standard corank-one Whitney criterion [16] says that such a germ is a fold exactly when its kernel is transverse to the singular curve. Lemma 7.1 therefore identifies precisely the fold points.

Let x_0 be a candidate cusp, so $V_{eee} = 0$ and, by Lemma 7.2, also $c_4 \neq 0$; the reduced potential is then $V(0) + c_4\xi^4 + O(\xi^5)$, of type A_3.

It remains to verify that Θ_σ has an ordinary cusp. Let $\eta(\xi)$ be the solution of $V_f = 0$ used above and set $\mathfrak{c}(\xi) = \xi e + \eta(\xi) f$. If $\mathfrak{g}(\xi) = V(\mathfrak{c}(\xi))$ then $\mathfrak{g}'(\xi) = V_e(\mathfrak{c}(\xi))$, so

$$\nabla_P V_{q(y_0)}(\mathfrak{c}(\xi)) = (4c_4\xi^3 + O(\xi^4),\, 0)$$

in the (e, f) components. Put $\mathcal{A}_0 = \mathcal{A}(x_0)$. At $x = \mathfrak{c}(\xi)$, equation (7.1) with $y = y_0$ gives

$$\mathcal{A}(\mathfrak{c}(\xi))\{y_0 - \Theta_\sigma(\mathfrak{c}(\xi))\} = \nabla_P V_{q(y_0)}(\mathfrak{c}(\xi)).$$

Since $\mathcal{A}(\mathfrak{c}(\xi))^{-1} = \mathcal{A}_0^{-1} + O(\xi)$, the preceding $O(\xi^3)$ expansion yields

$$\Theta_\sigma(\mathfrak{c}(\xi)) - y_0 = -4c_4\xi^3\mathcal{A}_0^{-1}(1, 0) + O(\xi^4). \tag{7.4}$$

By (7.2), $\operatorname{im} d\Theta_{\sigma,x_0} = \mathcal{A}_0^{-1} \operatorname{im} H(x_0) = \mathbb{R}\,\mathcal{A}_0^{-1}(0, 1)$, so the cubic vector in (7.4) is transverse to the rank-one image of $d\Theta_{\sigma,x_0}$.

We spell this out in rank coordinates. Since $d\Theta_{\sigma,x_0}$ has rank one, choose target coordinates whose first axis is $\operatorname{im} d\Theta_{\sigma,x_0}$ and then source coordinates (s, t) in which the map germ becomes $\Theta_\sigma - y_0 = (s, \mathsf{h}(s, t))$, with the kernel equal to the t-axis; the Jacobian is h_t, and $d\mathsf{h}(0) = 0$. Kernel tangency gives $\mathsf{h}_{tt}(0) = 0$, while simple vanishing of the Jacobian gives $\mathsf{h}_{st}(0) \neq 0$. In these coordinates $t(\mathfrak{c}(\xi)) = \chi\xi + O(\xi^2)$ with $\chi \neq 0$, because $\mathfrak{c}'(0) = e$ spans the kernel. Moreover, $s(\mathfrak{c}(\xi)) = O(\xi^3)$ because s is the first component of $\Theta_\sigma - y_0$ and (7.4) applies. Since $d\mathsf{h}(0) = 0$ and $\mathsf{h}_{tt}(0) = 0$, the transverse component in (7.4) has cubic coefficient $\chi^3\mathsf{h}_{ttt}(0)/6$; hence $\mathsf{h}_{ttt}(0) \neq 0$. Whitney's normal form for such a germ [16], [7, Ch. VI, Thm. 2.2], puts it into the ordinary cusp form

$$\mathsf{W}(s, t) = (s,\ \mathsf{a}t^3 + \mathsf{b}st), \qquad \mathsf{ab} \neq 0. \tag{7.5}$$

The source and target changes may be chosen orientation preserving. Indeed, replacing the source coordinate t by $-t$ reverses only the source-chart orientation and changes (a, b) to $(-\mathsf{a}, -\mathsf{b})$; replacing the second target coordinate by its negative does the same for the target-chart orientation. Thus the two orientations can be corrected independently while retaining (7.5). $\square$

7.2 The cusp count

Proposition 7.4 (Exactly three cusps)**.** *Every fold circle carries exactly three cusps. The zero set of the π-antiperiodic function ρ in (6.1) has exactly three classes modulo π, all simple. Equivalently, along any lift of one once-around projective circuit, ρ changes sign at exactly three zeros.*

Proof. Orient $\mathbb{RP}^1$ by increasing angle modulo π, parametrize $\partial\Omega$ positively, and define

$$\mathsf{T}, \mathsf{K} : \partial\Omega \longrightarrow \mathbb{RP}^1, \qquad \mathsf{T}(x) = T_x\partial\Omega, \qquad \mathsf{K}(x) = \ker d\Theta_{\sigma,x}.$$

Identify $\mathbb{RP}^1$ with $\mathbb{R}/\pi\mathbb{Z}$. For local angle lifts α and β of T and K, respectively, the expression

$$\mathsf{F}(x) = e^{2i(\alpha(x) - \beta(x))}$$

defines a global circle map. By Lemma 7.1 and Proposition 7.3, $\mathsf{F}(x) = 1$ exactly at the cusp parameters. At such a parameter put $\delta = \alpha - \beta$ and $\epsilon = \operatorname{sign} \delta'$, where the derivative is taken in a positive local boundary parameter.

The turning-number theorem for the positively oriented Jordan curve $\partial\Omega$ gives $\deg \mathsf{T} = 2$. By (3.12) a lift of ψ decreases by 2π around the boundary, and by Lemma 2.3 together with (7.2) one has $\mathsf{K}(x) = \ker H(x) = \mathbb{R}\, ie^{i\psi(x)/2}$, of degree -1. Consequently, $\deg \mathsf{F} = \deg \mathsf{T} - \deg \mathsf{K} = 3$.

The computation below shows that 1 is a regular value of F. Thus its preimage is finite, and the signed-preimage formula gives

$$\sum_{\text{cusps}} \epsilon = \deg \mathsf{F} = \deg \mathsf{T} - \deg \mathsf{K} = 2 - (-1) = 3. \tag{7.6}$$

It remains to show that no signs cancel. The map Θ_σ is a local diffeomorphism on the connected disc Ω, so its Jacobian has constant nonzero sign there. Reverse the orientation of the affine target if necessary so that $\det d\Theta_\sigma > 0$ in Ω. Since H is positive definite in Ω, (7.2) gives $\det \mathcal{A} = \det H / \det d\Theta_\sigma > 0$ in Ω; invertibility and continuity therefore give $\det \mathcal{A} > 0$ on $\partial\Omega$ as well. At a cusp x_0 with $y_0 = \Theta_\sigma(x_0)$, (7.1) reads $\nabla_P V_{q(y_0)}(x) = -\mathcal{A}(x)\{\Theta_\sigma(x) - y_0\}$.

The normal form (7.5) shows that x_0 is an isolated preimage of y_0, so both sides have a well-defined local degree. Both $\mathcal{A}(x)$ and $-I$ lie in $GL^+(2,\mathbb{R})$, which is connected, so after shrinking an isolating neighbourhood of x_0 the matrix field $-\mathcal{A}(x)$ is homotopic to the identity through $GL^+(2,\mathbb{R})$-valued fields; multiplication by this homotopy creates no boundary zero, whence $\deg_{x_0}(\Theta_\sigma - y_0) = \deg_{x_0} \nabla_P V_{q(y_0)}$.

The local degree of a gradient is invariant under right equivalence. Indeed, if $V = G \circ \Phi$, then $\nabla V = D\Phi^{\mathsf{T}}(\nabla G) \circ \Phi$; the orientation sign of Φ occurs once through precomposition and once through multiplication by $D\Phi^{\mathsf{T}}$, and therefore cancels. By the splitting lemma, the germ of $V_{q(y_0)}$ at x_0 is right equivalent to $c_4\xi^4 + \frac{\kappa}{2}\eta^2$, whose gradient $(4c_4\xi^3, \kappa\eta)$ has local degree $\operatorname{sign}(\kappa c_4) = -1$ by Lemma 7.2. Hence $\deg_{x_0}(\Theta_\sigma - y_0) = -1$.

Having fixed this target orientation, choose the orientation-preserving Whitney coordinates guaranteed by Proposition 7.3. In these coordinates the Jacobian is $J_{\mathsf{W}} = 3\mathsf{a}t^2 + \mathsf{b}s$, and it is positive on the side corresponding to Ω. For a sufficiently small regular value $(0, v)$, the unique nearby preimage is $(0, t_v)$ with $\mathsf{a}t_v^3 = v$; the Jacobian there has sign $\operatorname{sign}(3\mathsf{a}t_v^2) = \operatorname{sign} \mathsf{a}$. Hence $\deg_0 \mathsf{W} = \operatorname{sign} \mathsf{a}$, and therefore $\mathsf{a} < 0$.

The singular curve is $s = -3\mathsf{a}t^2/\mathsf{b}$. Put

$$\gamma(\zeta) = (s(\zeta), t(\zeta)) = \Big(-\frac{3\mathsf{a}}{\mathsf{b}}\zeta^2,\ -\operatorname{sign}(\mathsf{b})\,\zeta\Big).$$

Along this curve, $\nabla J_{\mathsf{W}}(\gamma(\zeta)) = |\mathsf{b}|\,(-t_\zeta, s_\zeta)$.

Thus the left normal points into $\{J_{\mathsf{W}} > 0\}$, proving that γ is the positive-boundary parametrization. The local coincidence sign is invariant under an orientation-preserving source-coordinate change: the induced map of $\mathbb{RP}^1$ is orientation preserving, and at a coincidence the variation of the coordinate change acts equally on the two line fields. We may therefore compute ϵ in the (s,t) coordinates. The kernel of $d\mathsf{W}$ along γ is the constant t-axis, so

$$\delta'(0) = \frac{\det(\gamma'(0), \gamma''(0))}{|\gamma'(0)|^2} = -\frac{6\mathsf{a}}{|\mathsf{b}|} \neq 0.$$

It follows that 1 is a regular value of F and that $\epsilon = -\operatorname{sign} \mathsf{a} = +1$ at every cusp. With (7.6), this gives exactly three cusps.

Finally, Proposition 6.1 identifies $\partial\Omega$ diffeomorphically with $\mathbb{R}/\pi\mathbb{Z}$ through the projective normal angle θ mod π. A cusp is exactly a zero of ρ in (6.1), because

$$\Gamma'(\theta(t)) = \frac{1}{\theta_t}\, d\Theta_{\sigma, x(t)}(x_t)$$

vanishes precisely when the tangent lies in the kernel. Restricting (7.5) to its singular curve gives $\mathsf{W} = \big(-3\mathsf{a}\zeta^2/\mathsf{b},\ 2\mathsf{a}\operatorname{sign}(\mathsf{b})\zeta^3\big)$, whose second derivative at $\zeta = 0$ is nonzero. Because the target coordinate change is a local diffeomorphism and the first derivative vanishes, the corresponding caustic derivative satisfies $\Gamma_{\zeta\zeta} \neq 0$. At the cusp, $\Gamma_\zeta = 0$ and $\theta_\zeta \neq 0$, so

$$\Gamma_{\theta\theta} = \frac{\Gamma_{\zeta\zeta}}{\theta_\zeta^2} \neq 0.$$

On the other hand, differentiating (6.1) and using $\rho = 0$ there gives $\Gamma_{\theta\theta} = \rho'\mathbf{v}$. Hence $\rho' \neq 0$. Thus the π-periodic zero set of ρ has exactly three classes modulo π, all simple, and ρ changes sign at each one. Figure 2 shows a caustic with its three cusps. □

8 Three-sign-change envelopes are embedded

For a continuous real function ρ on a nonempty open interval I, define its alternation number by

$$\operatorname{alt}_I(\rho) = \sup\left\{ m \in \mathbb{Z}_{\geq 0} : \begin{array}{c} x_0 < \cdots < x_m \text{ in } I, \\ \rho(x_j)\rho(x_{j+1}) < 0 \quad (0 \leq j < m) \end{array} \right\}.$$

The value $m = 0$ is always attained, so the supremum is over a nonempty set. Zeros cannot occur among the sample points of a sequence with $m \geq 1$. Thus an isolated zero with the same sign on both sides creates no alternation, whereas an isolated zero with opposite constant signs on its two sides creates one. The value $+\infty$ is allowed.

Lemma 8.1. *Let $h \in C^2(\mathbb{R}/2\pi\mathbb{Z})$ satisfy $h(\theta + \pi) = -h(\theta)$, put $\rho = h + h''$, and define Γ by (6.1). Suppose that ρ is not identically zero on any nonempty open interval and that*

$$\sup_{t \in \mathbb{R}} \operatorname{alt}_{(t,t+\pi)}(\rho) \leq 3.$$

Then $\Gamma : \mathbb{R}/\pi\mathbb{Z} \to \mathbb{R}^2$ is injective.

Proof. Differentiating $h(\theta + \pi) = -h(\theta)$ shows that h' and h'' are π-antiperiodic, and hence so is ρ. Since $\mathbf{u}$ and $\mathbf{v}$ are also π-antiperiodic, (6.1) gives $\Gamma(\theta + \pi) = \Gamma(\theta)$; thus Γ descends to $\mathbb{R}/\pi\mathbb{Z}$.

Identify $\mathbb{R}^2$ with $\mathbb{C}$. Differentiating (6.1) gives $\Gamma'(s) = i\rho(s)e^{is}$, hence

$$\Gamma(b) - \Gamma(a) = i \int_a^b \rho(s) e^{is}\, ds. \tag{8.1}$$

Claim. If $I = (a, b)$ has length less than π and $\operatorname{alt}_I(\rho) \leq 1$, then the integral in (8.1) does not vanish.

If there is no alternation, all nonzero values of ρ have one sign, while $\cos(s - (a + b)/2) > 0$ on I because $|s - (a + b)/2| < \pi/2$. Therefore

$$\Re\left(e^{-i(a+b)/2} \int_a^b \rho(s) e^{is}\, ds \right) = \int_a^b \rho(s) \cos\!\left(s - \tfrac{a+b}{2}\right) ds$$

has a strict sign. If there is exactly one alternation, we first produce a cut. Let $\mathcal{P}_+ = \{\rho > 0\} \cap I$ and $\mathcal{P}_- = \{\rho < 0\} \cap I$. If neither $\sup \mathcal{P}_+ \leq \inf \mathcal{P}_-$ nor $\sup \mathcal{P}_- \leq \inf \mathcal{P}_+$ held, there would exist $p \in \mathcal{P}_+, n \in \mathcal{P}_-$ with $p < n$ and $p' \in \mathcal{P}_+, n' \in \mathcal{P}_-$ with $n' < p'$. If $n' < p$, then $n' < p < n$ is a $(-,+,-)$ sample; if $p < n'$, then $p < n' < p'$ is a $(+,-,+)$ sample. Thus either case would give $\operatorname{alt}_I(\rho) \geq 2$. Consequently one of the two order relations holds. Choose a cut $c \in [a, b]$ between the corresponding ordered sign sets and, after reversing the overall sign if necessary, arrange that ρ is nonnegative on (a,c) and nonpositive on (c,b). Since $b-a<\pi$, the weight $-\sin(s-c)$ has exactly the same sign pattern, so

$$\Re\left(e^{-i(c-\pi/2)}\int_a^b \rho(s)e^{is}\,ds\right)=\int_a^b -\rho(s)\sin(s-c)\,ds$$

also has a strict sign. Strictness in both cases follows from continuity and the hypothesis that ρ vanishes on no open interval. This proves the claim.

Suppose now that $\Gamma(a)=\Gamma(b)$ for distinct projective parameters, and choose lifts with $0<b-a<\pi$. Since $\Gamma(a+\pi)=\Gamma(a)$, equation (8.1) vanishes on both (a,b) and $(b,a+\pi)$, and both intervals have length less than π. By the claim each carries at least two alternations, so each contains three interior sample points with alternating signs. If the terminal sign of the first sample and the initial sign of the second are opposite, their concatenation has five alternations. If those signs agree, deleting either one of the two join points leaves a five-point sample with four alternations. Both cases contradict the hypothesis on $(a,a+\pi)$. □

Corollary 8.2 (Jordan caustics)**.** *For each of the four discs Ω, let σ be the sign vector of its strict chamber. Then the affine caustic $\Gamma_\Omega:=\Theta_\sigma(\partial\Omega)\subset\mathbb{R}^2$ and the projective caustic $\mathcal{C}_\Omega:=\Theta(\partial\Omega)\subset\mathbb{RP}^2$ are Jordan curves, and their three cusp images are pairwise distinct.*

Proof. By Proposition 6.1, the support function h and $\rho=h+h''$ are real analytic, and the projective normal angle identifies $\mathbb{R}/\pi\mathbb{Z}$ diffeomorphically with $\partial\Omega$. Under this identification, the map Γ in (6.1) is $\Theta_\sigma|_{\partial\Omega}$ and has image Γ_Ω. By Proposition 7.4, ρ has exactly three simple zero classes modulo π; in particular, it vanishes on no open interval. Each alternation in an ordered sample forces, by the intermediate value theorem, a distinct zero between two consecutive sample points. Hence every open interval of length π has alternation number at most three.

Lemma 8.1 therefore makes Γ injective on $\mathbb{R}/\pi\mathbb{Z}$. Since its domain is compact and $\mathbb{R}^2$ is Hausdorff, Γ is a homeomorphism onto Γ_Ω. The inverse affine chart maps Γ_Ω homeomorphically onto $\mathcal{C}_\Omega$, so both are Jordan curves. The three cusp parameters are distinct modulo π by Proposition 7.4; injectivity therefore makes their images pairwise distinct. Here *Jordan* is meant topologically: Γ is not an immersion at its three ordinary cusps. □

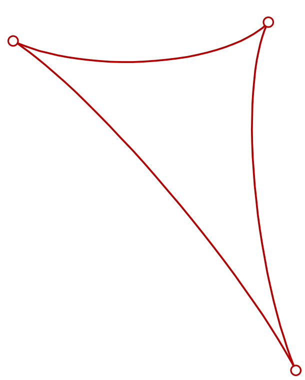

Figure 2: A numerical plot of the affine caustic $\Gamma_\Omega=\Theta_\sigma(\partial\Omega)$ of the interior disc of Figure 1, translated in the affine charge plane so that the barycentre of its three cusp images is at the origin. By Proposition 7.4 it has exactly three ordinary cusps (marked), all of the same coincidence sign, and by Corollary 8.2 it is a Jordan curve.

9 Fibres and the final count

All gradient indices and windings in this section are two-dimensional: they are taken in the site plane P in the noncollinear case and in a fixed meridian plane in the collinear case. We write $\operatorname{ind}_x \nabla V$ for the local degree of a planar gradient at an isolated zero. We also set

$$\mathfrak{N} = \#\operatorname{Crit}(V_q).$$

Proposition 9.1 (Fibre alternatives)**.** *Let the sites be noncollinear and put*

$$m = \#(\Theta^{-1}([q]) \cap \mathcal{R}), \qquad d = \#(\Theta^{-1}([q]) \cap \partial\mathcal{R}).$$

If $[q]$ lies on no caustic, then $m \le 1$ and $d = 0$. If $[q]$ lies on a caustic, then $m = 0$ and $d = 1$, and the corresponding degenerate equilibrium has planar gradient index $\iota \in \{0, -1\}$, namely 0 at a boundary fold and -1 at a boundary cusp.

Proof. Fix a disc Ω, let σ be the sign vector of its strict barycentric chamber, and work in the associated affine target chart. Orient Γ_Ω by the positive boundary orientation of $\partial\Omega$. Since $\overline{\Omega}$ lies in the strict chamber, $\Theta(\overline{\Omega}) \subset U_\sigma$; a charge ray outside U_σ therefore has no preimage in $\overline{\Omega}$. For a ray in U_σ, let y be its affine coordinate. If $y \notin \Gamma_\Omega$, then $(\Theta_\sigma|_{\overline{\Omega}})^{-1}(y)$ is compact and lies in Ω; it is discrete by regularity and hence finite. Moreover, the Jacobian of Θ_σ has constant nonzero sign on the connected disc Ω. The boundary formula for Brouwer degree therefore gives

$$\#(\Theta_\sigma^{-1}(y) \cap \Omega) = |\deg(\Theta_\sigma, \Omega, y)| = |\operatorname{wind}(\Gamma_\Omega, y)| \le 1. \tag{9.1}$$

The final inequality follows because Γ_Ω is a Jordan curve (Corollary 8.2). Now let $y \in \Gamma_\Omega$. Boundary injectivity gives exactly one boundary preimage. There is no interior preimage: if there were, its local inverse would persist for target points on both sides of the Jordan curve, and choosing a nearby point on the side with winding zero would give a nonempty fibre whose local degrees all have one sign, contradicting degree zero.

By Lemma 2.4, any two points of the same fibre that lie in $\overline{\mathcal{R}}$ belong to the same strict barycentric sign chamber. Proposition 3.5 identifies the portion of $\overline{\mathcal{R}}$ in each admissible chamber with one disc closure $\overline{\Omega}$; hence a fibre meets at most one of the four disc closures. Combining this observation with the off-caustic and on-caustic arguments above gives the stated alternatives; in particular, $[q]$ cannot lie on two caustics. Finally, Proposition 7.3 and the splitting normal forms of Section 7 give the planar gradient index at a boundary point. At a fold the potential germ is right equivalent to $\frac{V_{eee}}{6}\xi^3 + \frac{\kappa}{2}\eta^2$, with $V_{eee} \ne 0$, whose gradient has local degree 0. At a cusp it is right equivalent to $c_4\xi^4 + \frac{\kappa}{2}\eta^2$, whose gradient has local degree $\operatorname{sign}(\kappa c_4) = -1$ by Lemma 7.2. ☐

Remark 9.2. Proposition 9.1 determines ι exactly, but only the bound $\iota \le 1$ is used below. That weaker bound also follows, independently of Section 7, from Khimshiashvili's formula [8]; see also [2, Ch. I, §3]. If $f : (\mathbb{R}^2, 0) \to (\mathbb{R}, 0)$ is real analytic with an isolated critical point and $0 < \delta_{\mathrm{M}} \ll \varepsilon_{\mathrm{M}} \ll 1$ are Milnor data, then

$$\operatorname{ind}_0 \nabla f = 1 - \chi(F_-) \le 1, \qquad F_- = f^{-1}(f(0) - \delta_{\mathrm{M}}) \cap \overline{B}_{\varepsilon_{\mathrm{M}}}(0),$$

because F_- is a compact smooth one-manifold, possibly empty; each of its components is a circle or a compact interval, so $\chi(F_-) \ge 0$.

Proof of Theorem 1, noncollinear case. By Lemma 2.1 we may work entirely in P, and by the finite-critical-set hypothesis the zero set of $\nabla_P V_q$ consists of finitely many isolated points. No equilibrium lies on a site line, since $\lambda_k = 0$ would force $q_k = 0$ by (2.1); so every equilibrium lies in a strict chamber. By Proposition 3.5, an equilibrium outside $\overline{\mathcal{R}}$ satisfies $|\Xi| > 1/3$ and is therefore a regular saddle of planar index -1 by Lemma 2.3.

Apply the degree theorem to a sufficiently large closed disc after removing pairwise disjoint small discs about the three sites and isolating discs about the equilibria. Let w_∞ be the winding of $\nabla_P V_q$ on the positively oriented outer circle. On a counterclockwise circle of radius ε about a_i, the field is $-q_i\varepsilon^{-2}e^{i\theta} + O(1)$ and therefore has winding $+1$, independently of the sign of q_i. Each site circle has the opposite, clockwise orientation as an inner boundary, so its contribution is -1. Additivity of degree gives

$$\sum_{x\in\mathrm{Crit}(V_q)} \mathrm{ind}_x \nabla_P V_q = w_\infty - 3. \tag{9.2}$$

Let $\mathfrak{s}$ be the number of equilibria outside $\overline{\mathcal{R}}$. By Proposition 9.1 and (9.2) there are two cases. Every point counted by m has index $+1$ by Lemma 2.3, and every point counted by $\mathfrak{s}$ has index -1. If $d = 0$, then $m \le 1$ and $\mathfrak{N} = m + \mathfrak{s}$, while $m - \mathfrak{s} = w_\infty - 3$. Consequently,

$$\mathfrak{N} = 2m + 3 - w_\infty \le 5 - w_\infty. \tag{9.3}$$

If $d = 1$, then $m = 0$, the unique boundary point contributes ι, and $\mathfrak{N} = \mathfrak{s}+1$, while $\iota-\mathfrak{s} = w_\infty-3$. Consequently,

$$\mathfrak{N} = \iota + 4 - w_\infty \le 5 - w_\infty. \tag{9.4}$$

It remains to compute the outer winding in (9.2). Put $\mathsf{Q} = \sum_i q_i$ and $\mathbf{p} = \sum_i q_i a_i$. Uniformly for $x = R\omega$ with $|\omega| = 1$,

$$\nabla_P V_q(R\omega) = -\frac{\mathsf{Q}}{R^2}\omega + \frac{\mathbf{p} - 3(\mathbf{p}\cdot\omega)\omega}{R^3} + O(R^{-4}). \tag{9.5}$$

If $\mathsf{Q} \neq 0$, the leading field in (9.5) is radial and $w_\infty = 1$; then (9.3)–(9.4) give $\mathfrak{N} \le 4$. If $\mathsf{Q} = 0$, affine independence implies $\mathbf{p} \neq 0$, for otherwise (q_1, q_2, q_3) would be a nonzero affine dependence among the sites. After an orientation-preserving rotation and division by the positive scalar $|\mathbf{p}|$, neither of which changes winding, assume that $\mathbf{p} = 1$. For $\omega = e^{i\theta}$,

$$\mathbf{p} - 3(\mathbf{p}\cdot\omega)\omega = -\tfrac{1}{2}(1 + 3e^{2i\theta}).$$

The curve $1 + 3e^{2i\theta}$ traverses twice counterclockwise the circle of radius 3 centered at 1. The origin lies in its interior but not on its image, so the curve is nonvanishing and has winding 2; multiplication by $-1/2$ does not change the winding. Thus $w_\infty = 2$ and $\mathfrak{N} \le 3$. In both cases the leading field has a positive minimum norm on the unit circle. The uniform remainder in (9.5) is therefore joined to the leading field by a nonvanishing straight-line homotopy for all sufficiently large R, which justifies the winding computations. $\square$

Remark 9.3 (The zero-sum case). Let the sites be noncollinear with $\mathsf{Q} = 0$, so $w_\infty = 2$ and (9.3), (9.4) read $\mathfrak{N} = 2m + 1$ when $d = 0$ and $\mathfrak{N} = \iota + 2$ when $d = 1$, respectively. Since $m \le 1$ and $\iota \in \{0, -1\}$, it follows that

$$\mathfrak{N} = 3 \iff m = 1 \text{ and } d = 0.$$

At every equilibrium $q = \varsigma\,\vartheta(x)$ for some $\varsigma \neq 0$. Nonzero rescaling preserves the zero-sum condition, so we use the canonical representative $q^{\mathrm{can}}(x) := \vartheta(x)$ and put

$$\mathfrak{m}_k(x) = \sum_i \lambda_i(x) r_i(x)^k.$$

Then

$$\mathfrak{m}_0 = \sum_i \frac{q_i^{\mathrm{can}}(x)}{r_i^3} = \sum_i \lambda_i = 1, \qquad \mathfrak{m}_2 = V_{q^{\mathrm{can}}(x)}(x) = R_c^2 - |x-O|^2, \qquad \mathfrak{m}_3 = \sum_i q_i^{\mathrm{can}}(x).$$

Thus the charge ray $\Theta(x)$, represented by $q^{\mathrm{can}}(x)$, is zero-sum exactly on the locus $\{\mathfrak{m}_3 = 0\}$. In particular, the equivalence above gives the necessary condition

$$\mathsf{Q} = 0, \quad \mathfrak{N} = 3 \quad \Longrightarrow \quad \exists x \in \mathcal{R}: \ \mathfrak{m}_3(x) = 0. \tag{9.6}$$

On the interior disc every $\lambda_i > 0$, so $\mathfrak{m}_3 > 0$ there; only the three edge discs can contribute. Fix an edge disc and, after a cyclic relabelling, assume $\lambda_1 < 0 < \lambda_2, \lambda_3$. The following hold throughout $\overline{\Omega}$:

(i) $\mathfrak{m}_0 = 1$;

(ii) $\mathfrak{m}_1 > 0$: the three nonzero vectors $\lambda_i u_i$ sum to zero and cannot be collinear, since that would make the three sites collinear. Thus $|\lambda_1| r_1, \lambda_2 r_2, \lambda_3 r_3$ are the side lengths of a nondegenerate triangle, and $|\lambda_1| r_1 < \lambda_2 r_2 + \lambda_3 r_3$;

(iii) $\mathfrak{m}_2 < 0$, by Lemma 2.4.

These three do not by themselves force $\mathfrak{m}_3 < 0$. After a common positive rescaling of all distances, normalize $r_1 = 1$, write $a = r_2$ and $b = r_3$, and consider the system $\mathfrak{m}_0 = 1$, $\mathfrak{m}_1 = \mathfrak{m}_2 = 0$. Since $1, a, b$ are distinct, its unique solution is

$$\lambda_1 = -\frac{ab}{(1-a)(b-1)}, \qquad \lambda_2 = \frac{b}{(1-a)(b-a)}, \qquad \lambda_3 = \frac{a}{(b-a)(b-1)}.$$

For $0 < a < 1 < b$ these coordinates have the required signs, and direct substitution gives $\mathfrak{m}_3 = ab > 0$. Because $\mathfrak{m}_1 = 0$, the weighted lengths satisfy a triangle equality, so this is a degenerate boundary datum rather than a noncollinear realization. In any noncollinear realization, (2.5) shows that $\mathfrak{m}_2 = 0$ forces $|\Xi| = 1$; thus the constraint $|\Xi| \le 1/3$ is essential. Even the strict moment inequalities are insufficient. For example, take $(r_1, r_2, r_3) = (1, 1/2, 2)$ and, for sufficiently small $\varepsilon > 0$, perturb the corresponding barycentric coordinates to

$$(\lambda_1, \lambda_2, \lambda_3) = \left(-2 + \frac{7\varepsilon}{5}, \frac{8}{3} - \varepsilon, \frac{1}{3} - \frac{2\varepsilon}{5}\right).$$

Then $\mathfrak{m}_0 = 1$, $\mathfrak{m}_1 = \varepsilon/10 > 0$, $\mathfrak{m}_2 = -9\varepsilon/20 < 0$, and $\mathfrak{m}_3 = 1 - 77\varepsilon/40 > 0$. The weighted lengths obey the strict triangle inequalities for small ε (the inequality that was saturated at $\varepsilon = 0$ has slack $\varepsilon/10$), so the data are realizable. Substitution in (9.7) below gives $1 - |\Xi|^2 = 9\varepsilon^2/25 + O(\varepsilon^3)$, so the realized data lie outside the edge disc for all sufficiently small $\varepsilon > 0$.

A Laplace representation narrows the possibilities. Fix $x \in \overline{\Omega}$ and put $\phi(s) = \sum_i q_i^{\mathrm{can}}(x) e^{-r_i(x)^2 s}$, suppressing x from the notation below. Using $\int_0^\infty s^\alpha e^{-r^2 s}\, ds = \Gamma(\alpha+1) r^{-2\alpha-2}$ gives

$$\int_0^\infty s^{1/2}\phi(s)\,ds = \frac{\sqrt{\pi}}{2}\mathfrak{m}_0 > 0, \qquad \int_0^\infty s^{-1/2}\phi(s)\,ds = \sqrt{\pi}\,\mathfrak{m}_2 < 0, \qquad \phi(0) = \mathfrak{m}_3.$$

We need only the following elementary three-term form of Descartes' rule. Combine equal decay rates, discard zero combined coefficients, and write $\phi(s) = \sum_{j=1}^{\nu} c_j e^{-\mu_j s}$ with $\mu_1 < \cdots < \mu_\nu$ and $\nu \le 3$. If $\nu = 3$, factoring $e^{-\mu_1 s}$ leaves a function whose derivative is a two-term exponential sum and therefore has at most one zero; Rolle's theorem gives at most two zeros of ϕ. If the coefficient sequence has at most one sign variation, the zero-variation case has no zero. With exactly one variation and $\nu = 3$, the patterns, up to an overall sign, are $(+,+,-)$ and $(+,-,-)$. Factoring $e^{-\mu_3 s}$ in the first case and $e^{-\mu_1 s}$ in the second leaves a strictly increasing function, so there is at most one zero. The cases $\nu \le 2$ are immediate. Thus the number of sign changes of ϕ on $(0,\infty)$ is at most the number of sign variations of its ordered coefficient sequence, and in particular is at most two.

If ϕ has no sign change, the two weighted integrals above have the same weak sign, a contradiction. If its sign pattern begins with $-$, then $\mathfrak{m}_3 = \phi(0) \le 0$. Suppose instead that the pattern is $(+,-)$, with its change at s_*. Put $F(s) = s^{-1/2}\phi(s)$. Then $sF(s) < s_*F(s)$ for every $s \ne s_*$ at which $\phi(s) \ne 0$, and hence

$$\int_0^\infty s^{1/2}\phi(s)\,ds < s_* \int_0^\infty s^{-1/2}\phi(s)\,ds < 0,$$

contrary to $\mathfrak{m}_0 = 1$. Hence, if $\mathfrak{m}_3 > 0$, the only compatible pattern is $(+,-,+)$. Two sign changes of ϕ force $\nu = 3$ and two coefficient sign variations. Thus the three distances are distinct, and the charge whose sign differs from the other two is at the middle distance. When $\mathfrak{m}_3 = 0$, a pattern beginning with $-$ is not excluded by this argument, so equality remains a separate possibility.

We do not know how to exclude these remaining cases in closed form. In view of (9.6), the issue is a four-parameter semialgebraic feasibility problem. Indeed $\sum_i \lambda_i u_i = 0$ determines the vectors u_i from (λ, r) up to a common orthogonal transformation (a rotation or reflection); reflection conjugates Ξ and therefore leaves $|\Xi|$ unchanged. Conversely, every (λ, r) with $\sum_i \lambda_i = 1$ for which the three lengths $|\lambda_i| r_i$ satisfy the strict triangle inequalities is realized by an actual noncollinear configuration: choose the vectors $\lambda_i u_i$ as the oriented sides of a nondegenerate triangle, and take $x = 0$ and $a_i = -u_i$. Set $B_i = \lambda_i^2 r_i^2$ and

$$\mathcal{J} = 2\sum_{i<j} B_i B_j - \sum_i B_i^2.$$

Heron's identity gives $\mathcal{J} = 16\Delta^2$, where Δ is the area of the triangle with oriented sides $\lambda_i u_i$. The determinant identity used in the proof of Lemma 2.4 also gives

$$\Delta = \frac{1}{2}\left|\det(\lambda_1 u_1, \lambda_2 u_2)\right| = S|\lambda_1\lambda_2\lambda_3|.$$

Combining $\mathcal{J} = 16S^2(\lambda_1\lambda_2\lambda_3)^2$ with (2.5) yields

$$1 - |\Xi|^2 = \frac{\mathcal{J}\,\mathfrak{m}_2}{\lambda_1\lambda_2\lambda_3\, r_1^2 r_2^2 r_3^2}. \tag{9.7}$$

After the common positive rescaling that normalizes $r_1 = 1$ and the substitution $\lambda_3 = 1 - \lambda_1 - \lambda_2$, the feasible set in $(\lambda_1, \lambda_2, r_2, r_3)$ is cut out by $r_2, r_3 > 0$, $\lambda_1 < 0 < \lambda_2, \lambda_3$, $\mathcal{J} > 0$, and $1 - |\Xi|^2 \ge 8/9$. Candidate zero-sum data satisfy in addition the polynomial equation $\mathfrak{m}_3 = 0$. This exact formulation isolates the remaining obstruction and motivates Conjecture 9.4, which is consistent with the collinear zero-sum case, where $M_0 = 0$ forces $\ell \ge 1$ and hence $\mathfrak{N} \le 2 - \ell \le 1$.

Conjecture 9.4. *For every noncollinear triple of sites, $\mathfrak{m}_3 < 0$ on the closure of each of the three edge discs. Consequently every zero-sum charge vector with finite critical set has $m = d = 0$, and its potential has exactly one equilibrium, a saddle.*

9.1 Collinear sites

Suppose finally that the sites are collinear, at $(h_i, 0, 0)$ on the first coordinate axis. An off-axis equilibrium would generate a full critical circle under rotation about that axis, so finiteness forces every equilibrium onto the axis.

Fix a meridian plane P_{m} containing the axis, orient it, and identify it with $\mathbb{C}$ via $(x_1, x_2) \mapsto x_1 + ix_2$, so that the axis is the real axis. Since V_q is invariant under the reflection fixing P_{m}, its normal derivative vanishes identically on P_{m}; hence the zeros of $\nabla_{P_{\mathrm{m}}} V_q$ in P_{m} are exactly $\mathrm{Crit}(V_q) \cap P_{\mathrm{m}}$, which by the previous paragraph is all of $\mathrm{Crit}(V_q)$.

Local indices. Recenter an axial equilibrium at the origin, and write (r, θ) for polar coordinates in P_{m}, with θ measured from the positive axis. Axisymmetry and three-dimensional harmonicity give the convergent zonal expansion

$$V_q(r, \theta) - V_q(0) = \sum_{j \geq 1} \mathsf{c}_j r^j P_j(\cos\theta).$$

The series and its termwise derivatives converge uniformly on compact subsets of a ball about the origin containing no site. Criticality gives $\mathsf{c}_1 = 0$. The potential cannot be locally constant: otherwise real-analytic continuation on the connected complement of the sites would make it constant, contradicting its pole at a site. Let $k = \min\{j : \mathsf{c}_j \neq 0\} \geq 2$. For $\mathcal{Y}_k = r^k P_k(\cos\theta)$ the meridian gradient on the unit circle is

$$\nabla \mathcal{Y}_k(\theta) = e^{i\theta} g_k(\theta), \qquad g_k = kP_k(\cos\theta) - i \sin\theta\, P_k'(\cos\theta).$$

The Legendre polynomial P_k has exactly k simple roots, all in $(-1, 1)$ [13, Theorem 3.3.1]. The function g_k never vanishes: a simultaneous zero of its real and imaginary parts with $\sin\theta \neq 0$ would be a common zero of P_k and P_k', while at $\sin\theta = 0$ one has $P_k(\pm 1) \neq 0$. At every zero of $P_k(\cos\theta)$ we have $\Re g_k = 0$ and $(\Re g_k)' = -k \sin\theta P_k'(\cos\theta) = k\, \Im g_k$, so, at each such crossing,

$$\frac{d}{d\theta} \arg g_k = \frac{\Re g_k\, (\Im g_k)' - \Im g_k\, (\Re g_k)'}{|g_k|^2} = -k.$$

There are $2k$ such crossings on $0 \leq \theta < 2\pi$, all clockwise. Define the projectivized direction map

$$[g_k] : S^1 \longrightarrow \mathbb{RP}^1, \qquad e^{i\theta} \longmapsto \mathbb{R} g_k(\theta).$$

The crossings are precisely the transverse preimages of the vertical projective direction, so $\deg[g_k] = -2k$. Projectivization doubles the ordinary winding, and hence $\mathrm{wind}(g_k) = -k$. Since $e^{i\theta}$ has winding 1 and multiplication by the nonzero real coefficient c_k adds no winding, the local index is

$$\mathrm{ind}_0\, \nabla_{P_{\mathrm{m}}} V_q = 1 - k \leq -1.$$

The higher terms do not change the index. More precisely, uniformly in θ as $r \downarrow 0$,

$$r^{1-k} \nabla_{P_{\mathrm{m}}} V_q(re^{i\theta}) = \mathsf{c}_k \nabla \mathcal{Y}_k(e^{i\theta}) + o(1).$$

The leading field has a positive minimum norm, so the straight-line homotopy to the rescaled full gradient is nonvanishing for sufficiently small r.

Winding at infinity. Put $M_j = \sum_i q_i h_i^j$. For $R > \max_i |h_i|$, the Legendre generating function and its termwise derivatives give

$$V_q(R,\theta) = \sum_{j\ge 0} M_j R^{-j-1} P_j(\cos\theta).$$

The Vandermonde matrix $(h_i^j)_{0\le j\le 2,\,1\le i\le 3}$ is invertible, and the charge vector is nonzero, so the first nonvanishing moment has order $\ell \in \{0,1,2\}$. The leading meridian gradient is a nonzero scalar multiple of $e^{i\theta}\widetilde{g}_\ell(\theta)$ with

$$\widetilde{g}_\ell = -(\ell+1)P_\ell(\cos\theta) - i\sin\theta\, P_\ell'(\cos\theta),$$

which never vanishes by the same argument as for g_k (and equals -1 when $\ell = 0$). At a root of $P_\ell(\cos\theta)$ one has $(\Re\widetilde{g}_\ell)' = -(\ell+1)\Im\widetilde{g}_\ell$, so $\frac{d}{d\theta}\arg\widetilde{g}_\ell = \ell+1 > 0$ at the crossing. The 2ℓ crossings are all counterclockwise; the same projective-direction count therefore gives $\mathrm{wind}(\widetilde{g}_\ell) = \ell$ and

$$w_\infty = \ell + 1.$$

More precisely, uniformly in θ as $R \to \infty$,

$$R^{\ell+2}\nabla_{P_{\mathrm{m}}} V_q(Re^{i\theta}) = M_\ell e^{i\theta}\widetilde{g}_\ell(\theta) + O(R^{-1}).$$

The leading field has positive minimum norm, so a nonvanishing straight-line homotopy shows that the remainder cannot alter the winding for sufficiently large R.

Proof of Theorem 1, collinear case. Apply the degree theorem in P_{m}. The finite critical set gives finitely many isolated zeros of $\nabla_{P_{\mathrm{m}}} V_q$. On a counterclockwise small circle the field has winding $+1$ about each site; the clockwise inner-boundary orientation therefore subtracts these three windings. Hence

$$\sum_{x\in\mathrm{Crit}(V_q)} \mathrm{ind}_x\, \nabla_{P_{\mathrm{m}}} V_q = w_\infty - 3 = \ell - 2.$$

Every summand is at most -1, so $\mathfrak{N} \le 2-\ell \le 2$. The collinear case is therefore stronger than required, and the proof of Theorem 1 is complete. □

10 Computer-assisted exact verification

The directory `certificates/` in the public github repository `github.com/shivakintali/Maxwell3` contains the exact certificates and a README file.

Scope of the exact certificates. The canonical runner invokes seven scripts. The certificate `certificates/interior_jacobian.py` verifies (3.2), (3.3), and (3.4), including the Ravi expansion and the thirty AM–GM circuits. The certificate `certificates/edge_fold.py` verifies (3.8), (3.9)–(3.11), and the equilateral eliminant, critical values, and Hessian data used in the proof of Proposition 3.4; it also verifies the strict-moment and shape-deficit calculation in Remark 9.3. The certificates `certificates/lami_integer.py`, `certificates/lami_symbolic.py`, and `certificates/lami_projective.py` collectively verify (5.5), (5.6), the affine compatibility needed in Step 2 of Proposition 5.1, (5.9)–(5.10), (5.11), the regularized system (5.12)–(5.13), and (5.14)–(5.15). Finally, `certificates/coulomb_derivatives.py` verifies the sourcewise derivative table in Section 7, and `certificates/cusp_quartic.py` verifies the kernel and Laurent-polynomial identities, (7.3), and the algebraic positivity certificates used in Lemma 7.2.

The scripts certify only the algebraic statements just listed. The arguments that use them—including the edge-fold regularity deduction, the edge-disc continuation, the global smooth-extension argument in Proposition 5.1, and the analytic, topological, and degree-theoretic deductions—are supplied in the text.

Files and canonical run. The source distribution contains the canonical certificate directory `certificates/`. Its `README.md` gives an equation-level manifest for the seven canonical scripts. The file `cusp_tangent_chart.py` is supplementary exploratory material and is not invoked by `run_all.py`. Assuming that `.venv/` does not already exist, the following POSIX-shell commands, run from the manuscript directory, create a fresh virtual environment with the pinned package versions and execute the canonical suite:

```
python3.13 -m venv .venv
.venv/bin/python -m pip install -r certificates/requirements.txt
.venv/bin/python -I certificates/run_all.py
```

In the canonical suite, every proof-critical equality is enforced by an `assert` statement or an explicit exception, and `run_all.py` propagates any failure as a nonzero exit status. The runner requires unoptimized, isolated execution under CPython 3.13.x and rejects SymPy or mpmath versions other than those pinned in `certificates/requirements.txt`. A CPython patch release other than the audited 3.13.9 produces a warning rather than a failure.

Each canonical script constructs the relevant algebraic expressions in memory from formulas encoded directly in its source. Finite witness data, most notably the thirty integer AM–GM circuits, are likewise encoded in readable source. The suite uses exact differentiation and simplification over integers, rationals, algebraic numbers, polynomials, rational functions, and Laurent polynomials, including exact resultants and limits. It performs no floating-point arithmetic and loads no serialized symbolic data. The suite was audited with CPython 3.13.9, SymPy 1.14.0, and mpmath 1.3.0; these interpreter and library versions are recorded in `certificates/runtime.txt`.

Optional numerical diagnostic. The separately pinned NumPy dependency enables a floating-point consistency check of (3.3):

```
.venv/bin/python -m pip install -r certificates/requirements-sanity.txt
.venv/bin/python -I certificates/interior_jacobian.py --sanity
```

The second command reruns the exact interior-Jacobian certificate and adds a fixed-seed comparison of the direct and factored Jacobian formulas at 2,000 sample points, together with a sampled negativity check. This diagnostic was audited with NumPy 2.3.5; it is not used in the proof. Likewise, the numerical plots in Figures 1 and 2 are illustrative and play no logical role.

A The interior Jacobian certificate

Recall from the proof of Proposition 3.2 that $X = (\lambda_1, \lambda_2, \lambda_3, y_1, y_2, y_3)$ and $X^\nu = \prod_{j=1}^{6} X_j^{\nu_j}$. The polynomial $\mathcal{V}_{\mathrm{Ravi}}$ has 1578 nonzero monomials, exactly thirty of which have negative coefficients. Table 1 gives one circuit for each of them. Its rows are ordered by $r = 1, \dots, 30$; a row records the positive weight n_r and the exponent vectors $\alpha_r, \gamma_r, \beta_r \in \mathbb{Z}^6_{\geq 0}$. The vectors β_r are distinct and exhaust the negative support, the coefficient of X^{β_r} is $-\mathsf{n}_r$, and X^{α_r} and X^{γ_r} have positive coefficients in $\mathcal{V}_{\text{Ravi}}$.

For every row, $\alpha_r + \gamma_r = 2\beta_r$. Hence, for $X > 0$,

$$X^{\alpha_r} + X^{\gamma_r} - 2X^{\beta_r} = \left(\sqrt{X^{\alpha_r}} - \sqrt{X^{\gamma_r}}\right)^2 \geq 0.$$

Subtracting $\sum_{r=1}^{30} \frac{\mathsf{n}_r}{2}(X^{\alpha_r} + X^{\gamma_r} - 2X^{\beta_r})$ from $\mathcal{V}_{\text{Ravi}}$ leaves a polynomial $\mathcal{T}$ with exactly 1548 nonzero monomials. All its coefficients are positive integers, and the smallest is 16. Together with this exactly computed remainder, the thirty rows yield the coefficientwise identity (3.4); in particular, $\mathcal{T}(X) > 0$ and $\mathcal{V}_{\text{Ravi}}(X) > 0$ for $X > 0$. The calculation is reconstructed and checked in `certificates/interior_jacobian.py` using only exact arithmetic.

Table 1: The thirty AM–GM circuits of (3.4).

n_r	α_r						γ_r						β_r					
448	5	5	1	0	6	0	7	1	3	2	4	0	6	3	2	1	5	0
448	5	1	5	0	0	6	7	3	1	2	0	4	6	2	3	1	0	5
448	4	5	2	0	6	0	6	1	4	2	4	0	5	3	3	1	5	0
448	4	2	5	0	0	6	6	4	1	2	0	4	5	3	3	1	0	5
448	1	7	3	4	2	0	5	5	1	6	0	0	3	6	2	5	1	0
448	1	6	4	4	2	0	5	4	2	6	0	0	3	5	3	5	1	0
448	2	4	5	0	0	6	4	6	1	0	2	4	3	5	3	0	1	5
448	1	4	6	4	0	2	5	2	4	6	0	0	3	3	5	5	0	1
448	2	5	4	0	6	0	4	1	6	0	4	2	3	3	5	0	5	1
448	1	3	7	4	0	2	5	1	5	6	0	0	3	2	6	5	0	1
448	1	5	5	0	0	6	3	7	1	0	2	4	2	6	3	0	1	5
448	1	5	5	0	6	0	3	1	7	0	4	2	2	3	6	0	5	1
192	6	4	1	0	6	0	8	2	1	2	4	0	7	3	1	1	5	0
192	6	1	4	0	0	6	8	1	2	2	0	4	7	1	3	1	0	5
192	2	8	1	4	2	0	4	6	1	6	0	0	3	7	1	5	1	0
192	2	1	8	4	0	2	4	1	6	6	0	0	3	1	7	5	0	1
192	1	6	4	0	0	6	1	8	2	0	2	4	1	7	3	0	1	5
192	1	2	8	0	4	2	1	4	6	0	6	0	1	3	7	0	5	1
32	7	4	0	0	6	0	9	2	0	2	4	0	8	3	0	1	5	0
32	7	0	4	0	0	6	9	0	2	2	0	4	8	0	3	1	0	5
32	6	5	0	0	6	0	8	3	0	2	4	0	7	4	0	1	5	0
32	6	0	5	0	0	6	8	0	3	2	0	4	7	0	4	1	0	5
32	3	8	0	4	2	0	5	6	0	6	0	0	4	7	0	5	1	0
32	3	0	8	4	0	2	5	0	6	6	0	0	4	0	7	5	0	1
32	2	9	0	4	2	0	4	7	0	6	0	0	3	8	0	5	1	0
32	2	0	9	4	0	2	4	0	7	6	0	0	3	0	8	5	0	1
32	0	7	4	0	0	6	0	9	2	0	2	4	0	8	3	0	1	5
32	0	6	5	0	0	6	0	8	3	0	2	4	0	7	4	0	1	5
32	0	3	8	0	4	2	0	5	6	0	6	0	0	4	7	0	5	1
32	0	2	9	0	4	2	0	4	7	0	6	0	0	3	8	0	5	1

B The edge-fold polynomial $\mathcal{S}$

Here ℓ_i are the side lengths, and $s = \lambda_2/(\lambda_2 + \lambda_3)$ is the coordinate on the edge chamber $\lambda_1 < 0 < \lambda_2, \lambda_3$ used in Section 3. Equation (3.10) defines $\mathcal{S}$ without any undetermined scalar: it is the exact polynomial quotient in $\mathbb{Z}[s, \ell_1, \ell_2, \ell_3]$ obtained after removing the displayed factors from $\mathrm{Res}_t(\mathcal{L}_s, \mathcal{G}_0)$.

Write

$$\mathcal{S}(\ell_1,\ell_2,\ell_3;s)=\sum_{j=0}^{6}\mathcal{S}_j(\ell_1,\ell_2,\ell_3)s^j.$$

The polynomial satisfies $\deg_s \mathcal{S}=6$ over $\mathbb{Z}[\ell_1,\ell_2,\ell_3]$. Each coefficient $\mathcal{S}_j$ is homogeneous of degree 8 in (ℓ_1,ℓ_2,ℓ_3), and the leading coefficient $\mathcal{S}_6$ is not the zero polynomial. Consequently $\mathcal{S}$ has ordinary total degree 14 in (s,ℓ_1,ℓ_2,ℓ_3); it is not homogeneous in all four variables. Interchanging the two positive barycentric coordinates gives the exact reflection identity

$$\mathcal{S}(\ell_1,\ell_2,\ell_3;s)=\mathcal{S}(\ell_1,\ell_3,\ell_2;1-s).$$

This identity mixes the coefficients in the power basis in s and therefore is not a termwise symmetry of the list below. Expanding the following seven expressions and forming their displayed sum reproduces the exact quotient in (3.10). The zero remainder, degree statements, and reflection identity are checked in `certificates/edge_fold.py`.

$$\begin{aligned}
\mathcal{S}_6 =\ & (\ell_1-3\ell_2-3\ell_3)^2(\ell_1+3\ell_2+3\ell_3)^2\left(16\ell_1^2\ell_2\ell_3-3\ell_2^4+6\ell_2^2\ell_3^2-3\ell_3^4\right),\\
\mathcal{S}_5 =\ & -(\ell_1-3\ell_2-3\ell_3)(\ell_1+3\ell_2+3\ell_3)\big(48\ell_1^4\ell_2\ell_3-13\ell_1^2\ell_2^4-612\ell_1^2\ell_2^3\ell_3-846\ell_1^2\ell_2^2\ell_3^2\\
&-252\ell_1^2\ell_2\ell_3^3-5\ell_1^2\ell_3^4+157\ell_2^6+126\ell_2^5\ell_3-381\ell_2^4\ell_3^2-324\ell_2^3\ell_3^3\\
&+219\ell_2^2\ell_3^4+198\ell_2\ell_3^5+5\ell_3^6\big),\\
\mathcal{S}_4 =\ & 2\big(26\ell_1^6\ell_2\ell_3-11\ell_1^4\ell_2^4-723\ell_1^4\ell_2^3\ell_3-926\ell_1^4\ell_2^2\ell_3^2-273\ell_1^4\ell_2\ell_3^3-\ell_1^4\ell_3^4+282\ell_1^2\ell_2^6\\
&+4864\ell_1^2\ell_2^5\ell_3+12542\ell_1^2\ell_2^4\ell_3^2+12340\ell_1^2\ell_2^3\ell_3^3+5102\ell_1^2\ell_2^2\ell_3^4+724\ell_1^2\ell_2\ell_3^5\\
&+2\ell_1^2\ell_3^6-1711\ell_2^8-3087\ell_2^7\ell_3+3352\ell_2^6\ell_3^2+9585\ell_2^5\ell_3^3+2964\ell_2^4\ell_3^4\\
&-4725\ell_2^3\ell_3^5-3308\ell_2^2\ell_3^6-477\ell_2\ell_3^7-\ell_3^8\big),\\
\mathcal{S}_3 =\ & -2\ell_2\big(12\ell_1^6\ell_3-9\ell_1^4\ell_2^3-471\ell_1^4\ell_2^2\ell_3-427\ell_1^4\ell_2\ell_3^2-81\ell_1^4\ell_3^3+298\ell_1^2\ell_2^5\\
&+4030\ell_1^2\ell_2^4\ell_3+8036\ell_1^2\ell_2^3\ell_3^2+5780\ell_1^2\ell_2^2\ell_3^3+1602\ell_1^2\ell_2\ell_3^4+126\ell_1^2\ell_3^5\\
&-2209\ell_2^7-2211\ell_2^6\ell_3+6123\ell_2^5\ell_3^2+8541\ell_2^4\ell_3^3-147\ell_2^3\ell_3^4-3681\ell_2^2\ell_3^5\\
&-1175\ell_2\ell_3^6-57\ell_3^7\big),\\
\mathcal{S}_2 =\ & \ell_2\big(4\ell_1^6\ell_3-7\ell_1^4\ell_2^3-282\ell_1^4\ell_2^2\ell_3-142\ell_1^4\ell_2\ell_3^2-12\ell_1^4\ell_3^3+334\ell_1^2\ell_2^5\\
&+3444\ell_1^2\ell_2^4\ell_3+4706\ell_1^2\ell_2^3\ell_3^2+2060\ell_1^2\ell_2^2\ell_3^3+284\ell_1^2\ell_2\ell_3^4+12\ell_1^2\ell_3^5\\
&-3207\ell_2^7-1246\ell_2^6\ell_3+8432\ell_2^5\ell_3^2+6268\ell_2^4\ell_3^3-1843\ell_2^3\ell_3^4-1778\ell_2^2\ell_3^5\\
&-142\ell_2\ell_3^6-4\ell_3^7\big),\\
\mathcal{S}_1 =\ & \ell_2^3\big(\ell_1^4\ell_2+30\ell_1^4\ell_3-90\ell_1^2\ell_2^3-704\ell_1^2\ell_2^2\ell_3-482\ell_1^2\ell_2\ell_3^2-60\ell_1^2\ell_3^3\\
&+1241\ell_2^5-46\ell_2^4\ell_3-2370\ell_2^3\ell_3^2-632\ell_2^2\ell_3^3+481\ell_2\ell_3^4+30\ell_3^5\big),\\
\mathcal{S}_0 =\ & 8\ell_2^5\big(\ell_1^2\ell_2+7\ell_1^2\ell_3-25\ell_2^3+7\ell_2^2\ell_3+25\ell_2\ell_3^2-7\ell_3^3\big).
\end{aligned}$$

Acknowledgements: The author designed the details of the main construction, configurations and the proof strategy and manually prepared an initial draft. The author then used multiple AI tools (Claude, ChatGPT and two open-weight models with open-source harnesses) to find the relevant research papers and prompted these AI tools to work out the details of the equations and identify missing gaps. The author fixed those missing gaps and iteratively verified and expanded the proofs. When an AI tool was hallucinating, stuck, or going in the wrong direction, the author stopped that AI tool, corrected the intermediate `.md` files, added more specific new ideas and

switched to a different AI tool with more detailed fresh prompts. Equations written by one AI tool were critiqued, verified and expanded by a completely different AI tool in an iterative manner, till the author was satisfied with their correctness and details. The code in the `certificates/` directory was written by Claude Code and verified by the author. The author is solely responsible for the correctness of the proofs and the code.

References

[1] P. Arathoon, G. Ball, and M. D. Kvalheim, *The Maxwell conjecture is false*, arXiv:2607.27197v1 [physics.class-ph] (2026), https://arxiv.org/abs/2607.27197v1.

[2] V. I. Arnold, S. M. Gusein-Zade, and A. N. Varchenko, *Singularities of Differentiable Maps*, Vol. I, Monographs in Mathematics, vol. 82, Birkhäuser, Boston, 1985, https://doi.org/10.1007/978-1-4612-5154-5.

[3] Th. Bröcker and K. Jänich, *Introduction to Differential Topology*, Cambridge University Press, Cambridge, 1982.

[4] H. Edelsbrunner, C. Fillmore, and G. Oliveira, *Counting equilibria of the electrostatic potential*, Proc. Lond. Math. Soc. (3) **132** (2026), no. 5, Paper No. e70163, 32 pp., https://doi.org/10.1112/plms.70163.

[5] A. Gabrielov, D. Novikov, and B. Shapiro, *Mystery of point charges*, Proc. Lond. Math. Soc. (3) **95** (2007), no. 2, 443–472, https://doi.org/10.1112/plms/pdm012.

[6] A. Gabrielov, Dm. Novikov, T. Novikov, and B. Shapiro, *From 12 to 6: Sharpening the three-charge bound in Maxwell's problem*, arXiv:2607.28785v1 [math.CA] (2026), https://arxiv.org/abs/2607.28785v1.

[7] M. Golubitsky and V. Guillemin, *Stable Mappings and Their Singularities*, Graduate Texts in Mathematics, vol. 14, Springer, New York, 1973, https://doi.org/10.1007/978-1-4615-7904-5.

[8] G. N. Khimshiashvili, *On the local degree of a smooth mapping*, Soobshch. Akad. Nauk Gruzin. SSR **85** (1977), no. 2, 309–312 (in Russian).

[9] K. Killian, *A remark on Maxwell's conjecture for planar charges*, Complex Var. Elliptic Equ. **54** (2009), no. 12, 1073–1078, https://doi.org/10.1080/17476930903275946.

[10] J. C. Maxwell, *A Treatise on Electricity and Magnetism*, Vol. 1, 1st ed., Clarendon Press, Oxford, 1873, §113.

[11] J. C. Maxwell, *A Treatise on Electricity and Magnetism*, Vol. 1, 3rd ed., edited by J. J. Thomson, Clarendon Press, Oxford, 1892; unabridged republication, Dover Publications, New York, 1954, §113.

[12] R. Peretz, *Application of the argument principle to Maxwell's conjecture for three point charges*, Complex Var. Elliptic Equ. **58** (2013), no. 5, 715–725, https://doi.org/10.1080/17476933.2011.611939.

[13] G. Szegő, *Orthogonal Polynomials*, 4th ed., American Mathematical Society Colloquium Publications, vol. 23, American Mathematical Society, Providence, RI, 1975.

[14] Y.-L. Tsai, *Special cases of three point charges*, Nonlinearity **24** (2011), no. 12, 3299–3321, https://doi.org/10.1088/0951-7715/24/12/002.

[15] Y.-L. Tsai, *Maxwell's conjecture on three point charges with equal magnitudes*, Physica D **309** (2015), 86–98, https://doi.org/10.1016/j.physd.2015.07.007.

[16] H. Whitney, *On singularities of mappings of Euclidean spaces. I. Mappings of the plane into the plane*, Ann. of Math. (2) **62** (1955), 374–410, https://doi.org/10.2307/1970070.

[17] V. Zolotov, *Upper bounds for the number of isolated critical points via the Thom–Milnor theorem*, Anal. Math. Phys. **13** (2023), no. 5, Paper No. 81, 18 pp., https://doi.org/10.1007/s13324-023-00842-6.